ROCKETBORNE INSTRUMENTATION FOR THE MEASUREMENT OF ELECTRIC FIELDS - PAIUTE TOMAHAWK 10.312-3

L. Carl Howlett, et al

Utah State University

Prepared for:

Air Force Cambridge Research Laboratories
Defense Nuclear Agency

January 1975

AFCRL-TR-75-0023

ROCKETBORNE INSTRUMENTATION FOR THE MEASUREMENT OF ELECTRIC FIELDS - PAIUTE TOMAHAWK 10.312-3

by

L. Carl Howlett
Ronald J. Bell

SPACE SCIENCE LABORATORY
UTAH STATE UNIVERSITY
LOGAN, UTAH 84322

January 1975

Scientific Report No. 2 - HAES Report No. 11

This research was sponsored by the Defense Nuclear Agency under Subtask K43AAXHX604, entitled "E & F Region Ionization & Chemical Specie Measurements.

AIR FORCE CAMBRIDGE RESEARCH LABORATORIES
AIR FORCE SYSTEMS COMMAND
UNITED STATES AIR FORCE
HANSCOM AFB, MASSACHUSETTS 01731

Unclassified

Security Classification

DOCUMENT CONTROL DATA - R & D

Security classification of title, body of abstract and indexing annotation must be entered when the overall report is classified)

1. ORIGINATING ACTIVITY (Corporate author)
Space Science Laboratory
Utah State University
Logan, UT 84322

2a. REPORT SECURITY CLASSIFICATION
Unclassfied

2b. GROUP

3. REPORT TITLE
ROCKETBORNE INSTRUMENTATION FOR THE MEASUREMENT OF ELECTRIC FIELDS - PAIUTE-TOMAHAWK 10.312-3

4. DESCRIPTIVE NOTES (Type of report and inclusive dates)
Scientific Interim

5. AUTHOR(S) (First name, middle initial, last name)
L. Carl Howlett
Ronald J. Bell

6. REPORT DATE
January 1975

7a. TOTAL NO. OF PAGES
86

7b. NO. OF REFS
4

8a. CONTRACT OR GRANT NO.
F19628-74-C-0130

b. PROJECT NO.
CDNA-00-12

c.

d.

9a. ORIGINATOR'S REPORT NUMBER(S)
Scientific Report No. 2

9b. OTHER REPORT NO(S) (Any other numbers that may be assigned this report)
AFCRL-TR-75-0023

10. DISTRIBUTION STATEMENT
Approved for public release; distribution unlimited

11. SUPPLEMENTARY NOTES
HAES Report No. 11. This research was sponsored by the Defense Nuclear Agency under Subtask K43AAXHX604, entitled "E & F Region Ionization & Chemical Specie Measurements."

12. SPONSORING MILITARY ACTIVITY
Air Force Cambridge Research Laboratories (LI)
Hanscom AFB, Massachusetts 01731
Contract Monitor: Thomas D. Conley/OPR-1

13. ABSTRACT

On 18 April 1974, Paiute-Tomahawk 10.312-3 was launched from Poker Flat Research Range, Alaska, as part of the ICECAP 74B COMMOCAP program. Included in the payload were eight instruments to measure various auroral parameters. Of prime interest was the measurement of the magnitude and direction of the electric field in and over an auroral arc. Measurements were also made of the spectral energy distribution of primary and secondary particles, auroral light emission, and electron flux density and temperature.

Good data were received from seven of the eight experiments flown on PT10.312-3. Following data acquisition the recovery ststem was activated and the payload was recovered intact the following morning.

PRICES SUBJECT TO CHANGE

DD FORM 1 NOV 65 1473

Unclassified

Security Classification

14. KEY WORDS	LINK A		LINK B		LINK C	
	ROLE	WT	ROLE	WT	ROLE	WT
ICECAP - 74B						
COMMOCAP						
Auroral Measurements						
Electric Field Measuremetns						
Rocketborne Instrumentation						
Auroral Energy Inputs						

LIST OF CONTRIBUTORS - SCIENTISTS AND ENGINEERS

Kay D. Baker - Principal Investigator

D.A. Burt

L.C. Howlett

L.L. Jensen

G.K. LeBaron

N.C. Maynard (NASA)

W. Sharp (Univ. of Mich.)

RELATED CONTRACTS AND PUBLICATIONS

F19628-73-C-0048

F19628-72-C-0255

F19628-70-C-0302

F19628-69-C-0007

F19628-67-C-0275

AF19(628)-4995

Baker, K.D., G.D. Allred, and D.A. Burt, Rocket and satellite instrumentation for ionospheric measurements, *U of U Final Report, AFCRL 68-0270*, 72 pp., Contract No. AF19(628)-4995, Upper Air Research Laboratory, University of Utah, Salt Lake City, May 1968.

Baker, K.D., D.A. Burt, L.C. Howlett, and G.D. Allred, Rocket instrumentation for the study of a polar cap absorption event - PCA 69, *U of U Final Report, AFCRL 70-0281*, 270 pp., Contract No. F19628-67-C-0275, Upper Air Research Laboratory, University of Utah, Salt Lake City, April 1970.

Burt, D.A., and G.D. Allred, Rocket instrumentation for auroral measurements - Aerobee 3.756 and 3.759, *U of U Final Report, AFCRL 70-0658,* 193 pp., Contract 10.F19628-69-C-0007, Upper Air Research Laboratory, University of Utah, Salt Lake City, November 1970.

Baker, K.D., Rocketborne measurements of ionospheric distrubances, *USU Final Report, AFCRL 72-0601,* 39 pp., Contract No. F19628-70-C-*0302,* Space Science Laboratory, Utah State University, Logan, October 1972.

PREFACE

The High Altitude Effects Simulation (HAES) Program sponsored by the Defense Nuclear Agency since the early 1970 time period, comprises several groupings of separate, but interrelated technical activities, e.g., ICECAP (Infrared Chemistry Experiments-Coordinated Auroral Program). Each of the latter have the common objective of providing information ascertained as essential for the development and validation of predictive computer codes designed for use with high priority DoD radar, communications, and optical defensive systems.

Since the inception of the HAES Program, significant achievements and results have been described in reports published by DNA, participating service laboratories, and supportive organizations. In order to provide greater visibility for such information and enhance its timely applications, significant reports published since early calendar 1974 shall be identified with an assigned HAES serial number and the appropriate activity acronym (e.g., ICECAP) as part of the report title. A complete and current bibliography of all HAES reports issued prior to and subsequent to HAES Report No. 1, dated 5 February 1974 entitled, "Rocket Launch of a SWIR Spectrometer into an Aurora (ICECAP 72)", AFCRL Environmental Research Paper No. 466, is maintained and available on request from DASIAC, DoD Nuclear Information and Analysis Center, 816 State Street Santa Barbara, California 93102, Telephone (805) 965-0551.

This report is the second scientific report under Contract F19628-74-C-0130 and the eleventh report in the HAES series as referenced in Appendix D. The report is primarily concerned with the instrumentation of a Paiute-Tomahawk rocket which was launched to measure the magnitude and direction of electric fields in and over an auroral arc. In addition, other instruments aboard made measurements of electron flux, auroral light emissions, electron concentration and electron temperatures.

At Utah State University a number of individuals had specific responsibility for various phases of this project as indicated below:

Principal Investigator and Project Scientist	K.D. Baker
Project Engineer	L.C. Howlett
Langmuir Probe	L.C. Howlett D.A. Burt
Photometer	L.L. Jensen
Plasma Frequency Probe	G.K. LeBaron
Electron Spectrometer	P.C. Neal D.A. Burt
Particle Counter	L.C. Howlett
Payload Integration	L.C. Howlett
Field Operations	L.C. Howlett L.L. Jensen P.C. Neal
Documentation	R.J. Bell C. Clyde

TABLE OF CONTENTS

TABLE OF CONTENTS (cont.)

LIST OF ILLUSTRATIONS

LIST OF ILLUSTRATIONS (cont.)

LIST OF TABLES

INTRODUCTION

The Paiute-Tomahawk 10.312-3 payload was launched from Poker Flat Research Range on 18 April 1974 as part of the ICECAP 74B COMMOCAP program. This program involved the launching of four rocketborne payloads and was supported by extensive ground-based measurements. The PT10.312-3 payload was designed to measure the magnitude and direction of electric fields in and over an auroral arc. It also made measurements of the spectral energy distribution of primary and secondary particles, auroral light emissions, and electron density and temperature. The payload was recovered intact through the use of a recovery parachute.

PAYLOAD DESCRIPTION

Eight instruments to measure parameters in the auroral ionosphere were carried aloft aboard PT10.312-3. Table 1 lists these instruments, their sources and the measurement taken by each. Also listed in Table 1 are the supporting instruments and their functions. Figure 1 is a photograph showing the payload and instrumentation. The payload contained instruments which viewed parallel and at various angles with respect to the vehicle major axis and probes which extended from the payload into the ionospheric plasma. Fields of view were cleared and probes were extended after the payload had ascended above the dense portions of the atmosphere and after the protective doors and nosecone had been ejected. Figure 2 shows the fields of view and orientations for the various instruments.

Nine timed events occurred during the rocket flight. The sequence of events was as shown in Table 2. The despin unit reduced the vehicle motion to about 2 rps so that proper extension of the E-field probes could be accomplished (the increasing moment of inertia as the booms extended further slowed the vehicle spin rate to approximately 1.5 rps). Ejection of doors and nosetip cleared instrument fields of view and allowed for extension of booms and sensors. High voltage turn-on at 81 seconds eliminated the probability of arcing at critical pressures. After the measurements phase of the flight the payload was

TABLE 1

PAIUTE TOMAHAWK A10.312-3 PAYLOAD INSTRUMENTATION - ICECAP 74B

Instrument	Model/SN (Manufacturer)	Measurement or Function
Instrumentation for Measurements		
E-field probes electronics	Fairchild SN220 NASA #2	E-field
Electrostatic analyzer	ESA 202	Primary electron spectra
Langmuir probe	USU LP72-4	Electron density, temperature
Retarding potential analyzer (HARP)	Univ. of Mich.	Secondary electrons between 1 ev and 500 ev
Plasma frequency probe	USU PFP 73A-1	Electron density
Electron spectrometer	USU ES 73A-1	Secondary electron flux between 100 ev and 3 kev
Particle counter	USU PC 72B-4	Electron flux between 4.5 and 90 kev
Photometer	USU PM-A2-1	3914 A
Instrumentation for Support		
S-band telemetry		Data recovery
S-band beacon		Payload tracking
Gyro		Attitude determination
Recovery		Soft land payload
Despin		Despin to 1.5 rps
Magnetic aspect sensor	RAM 5C #7080	Magnetic pitch angle

Figure 1. Photograph of PT10.312-3 payload.

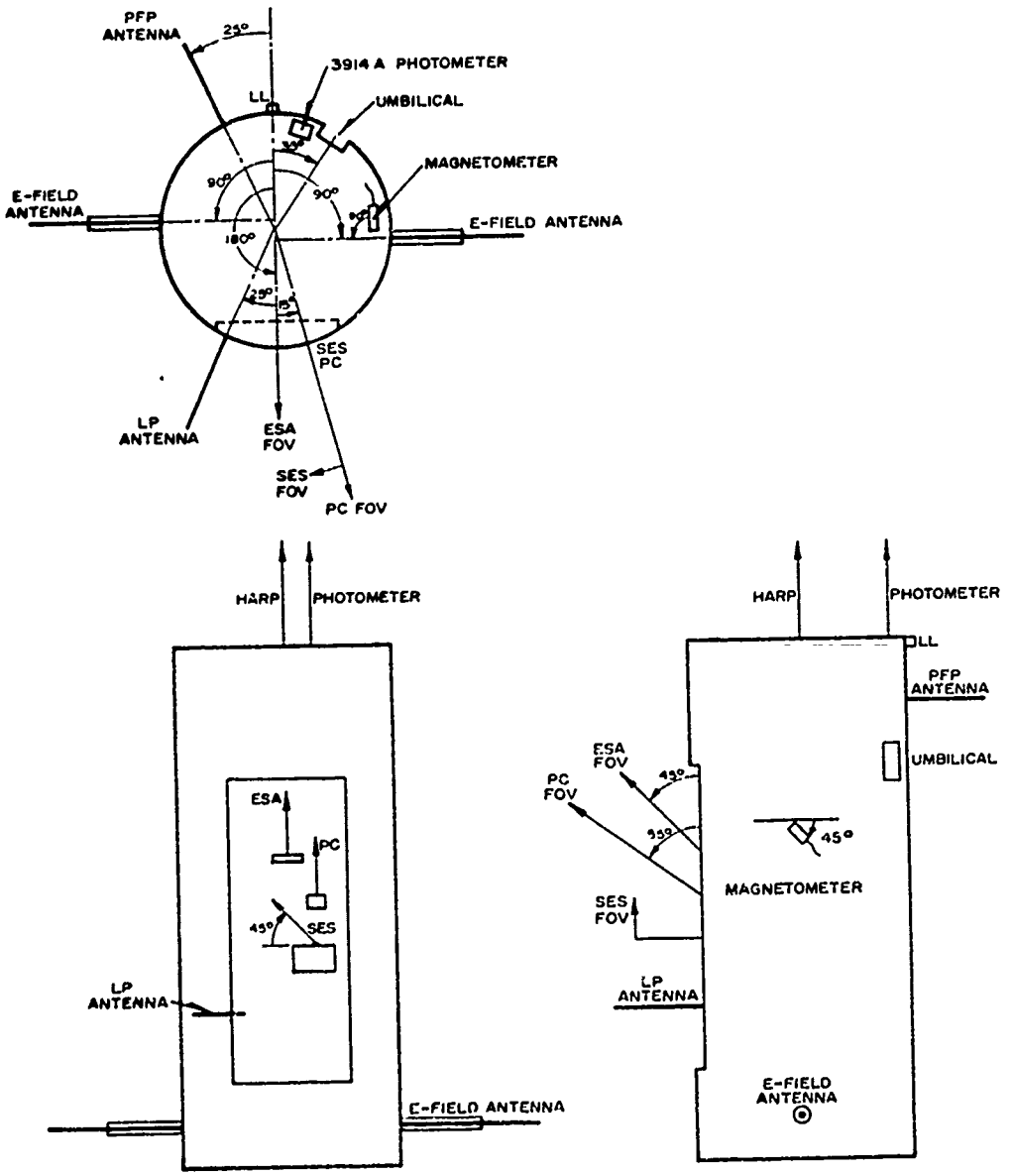

Figure 2. PT10.312-3 instrument orientation.

severed from the motor, high votlage was turned off and booms were severed in preparation for payload recovery via parachute.

TABLE 2

PAIUTE TOMAHAWK 10.312-3 SEQUENCE OF EVENTS

Event	Time (seconds)
Launch	0.0
Activate despin mechanism	54.0
Eject doors	68.1
Eject nosetip	71.3
Extended booms	74.6
Turn high voltage on (selected particle measuring instruments)	81.0
Sever payload from motor	330.0
Turn high voltage off	343.0
Cut booms off	343.0
Deploy parachute	410.0
Impact	925.0

PAYLOAD INSTRUMENTATION

Table 1 listed each instrument in the PT10.312-3 payload. This section of the report describes each of these instruments. Individual instrument calibrations are given in Appendix A.

Instrumentation for Measurements

Eight instruments were included in the payload to make measurements of auroral parameters. These included measurements of the magnitude and direction of the electric field, primary and secondary particle flux density and energy distributions, electron density and temperature, and auroral intensity and vertical emission profile at 3914A.

E-field Probe

The E-field experiment flown aboard PT10.312-3 was a joint effort of AFCRL, USU, and NASA. It provided measurements of magnitude and

direction of the earth's electric field. The instrument was provided by NASA for integration by USU in the payload. Data obtained are to be available to all participating agencies.

Figure 3 is a block diagram of the E-field probe. It uses the double floating probe method for measuring the electric field [*Maynard, 1971*]. After the payload passes through the dense lower atmosphere two cylindrical antennas are deployed. Each antenna is 6.2 m long with the inner one-half of the antenna insulated from the plasma. The distance between the midpoints of the two active elements is 9.3 m. The floating potentials on the probes are measured with high input impedance voltage followers and then differentially subtracted. The resultant signal is a measure of the total electric field as expressed by the following equation:

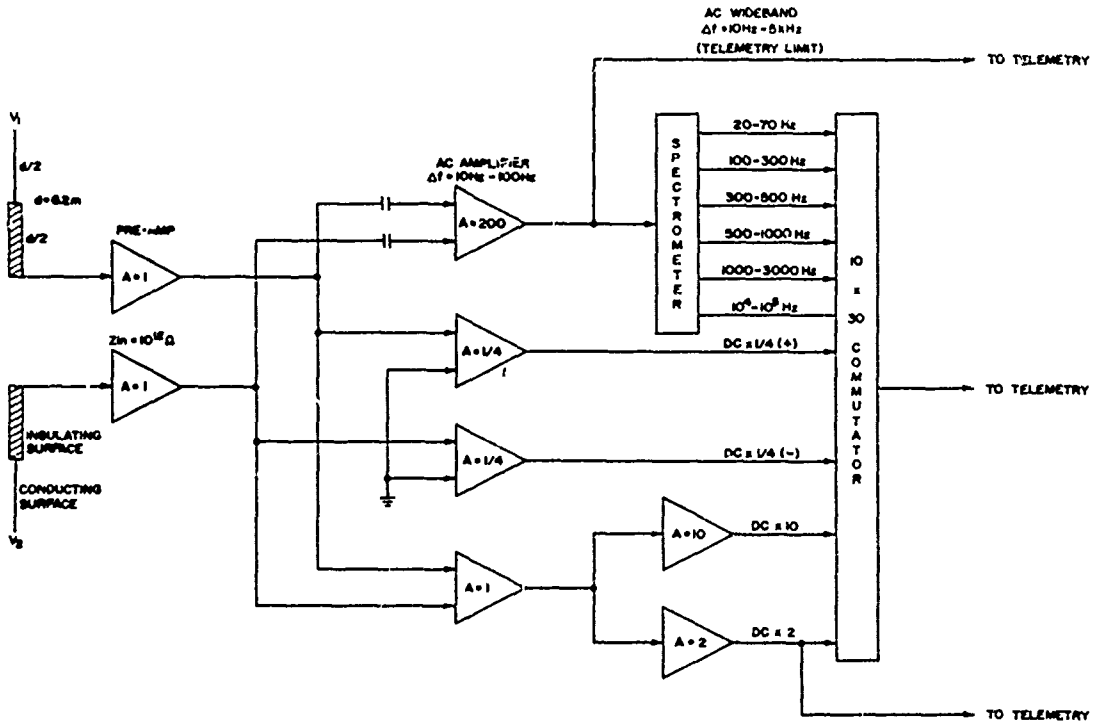

Figure 3. E-field probe block diagram.

$$\vec{E}_t = \vec{E} + \vec{v} \times \vec{B}$$

where $\vec{E}_t$ = the electric field measured by the probe

$\vec{E}$ = the ambient electric field

$\vec{v} \times \vec{B}$ = the electric field induced by the rocket motion ($\vec{v}$) through the magnetic field ($\vec{B}$)

Several data channels, as indicated in the block diagram, with different amplifications of the input signal are available. Data reduction and calibrations are to be provided by personnel from the NASA Goddard Space Flight Center.

Electrostatic Analyzer

The electrostatic analyzer (ESA) was provided by Visidyne Inc. and is used to obtain measurements of the incident spectrum of auroral electrons between 3 and 33 kev. It basically consists of a pair of concentric spherical octants (plates) with an exponentially decreasing positive voltage applied to the inner plate as shown in Figure 4.

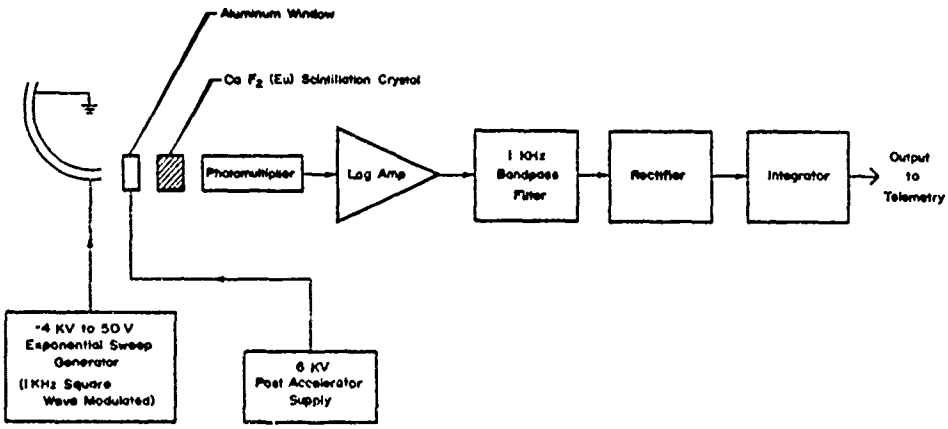

Figure 4. Electrostatic analyzer block diagram.

The outer plate is held at ground potential. Electrons entering between the plates with the proper angle and energy will pass through

the plates (without striking either surface) to an aluminum covered scintillator (europium activated calcium fluoride) which is coupled to a photomultiplier. The aluminum cover is used to prevent any effect due to incident light. It has an accelerating voltage applied to insure that low energy electrons will pass through and still have enough energy to produce a useable signal. The output signal of the photomultiplier is then a measure of the electron flux at energy E, where E is the energy at the center of the energy band for the applied sweep voltage. For this instrument, the geometrical parameters are such that E = 10 x sweep voltage.

The ESA flown aboard the E-field payload was essentially the same as those flown on previous auroral payloads [*Burt* and *Davis*, 1974]. It was mounted to view 45° from the rocket axis with a field of view of 6.4° x 16°. The main deviations from earlier versions came about because of suspected interference between the ESA and other instruments such as the Langmuir probe. On previous flights it appeared that as the ESA entered the high energy portion of its sweep it produced a discharge or in some way modified the vehicle potential, thereby upsetting the Langmuir probe and retarding potential analyzer. To minimize such effects from the ESA the plate with the high voltage sweep was shielded from the outside by a perforated metal shield. This hopefully would minimize the effective projected area of the analyzer plate. The ESA was further modified to spend a shorter time at the high energy portion of its sweep. The sweep period was also adjusted to approximately 2.4 seconds to avoid coincidence with the Langmuir probe sweep. Table 3 lists the ESA specifications.

The incident electron flux is computed from the following formula:

$$N_{(E)} = \frac{I}{S\zeta e(A\Omega)\ E\beta(E + eV_{PA} - 1.3\ E_c)}$$

where

$N_{(E)}[cm^2 sec\ ster\ ev]^{-1}$ = incident electron flux at energy E

$I[amp]$ = photomultiplier current measured at plate voltage V corresponding to electron energy bandpass centered at E

$S[\text{amp watts}^{-1}]$	=	scintillator and photomultiplier response (α-ray source)
ζ	=	energy dependent correction of scintillator response for electron deposition (Figure 5)
e[coulombs]	=	electron charge 1.6×10^{-19} coulombs
$A\Omega[\text{cm}^2 \text{ ster}]$	=	instrument geometric factor
ΔE[electron volts]	=	electron energy bandpass, FWHM
E	=	electron energy at center of bandpass
β	=	correction for loss by backscattering from the scintillator [*Sternglass*, 1954]
V_{PA}[volts]	=	post accelerator voltage
E_c[electron volts]	=	critical energy -- the energy of an electron with practical range equal to thickness of aluminum deposition (Figure 6)

TABLE 3

ELECTROSTATIC ANALYZER SPECIFICATIONS

Parameter	Value
Serial No.	202
Energy range	3-33 kev
Half power energy resolution	12%
Sweep period	2.4 sec
Time constant	165 ms
Modulation frequency	1 kHz
Field of view	$6.4 \times 16^{\circ}$
Geometric factor	9.3×10^{-2} cm^2 sr
Scintillator coating thickness	985 ± 50 A

The geometric factor and energy bandpass have been experimentally measured in the laboratory. The combined scintillator and photomultiplier sensitivity, S, is determined by measuring the combined response of the scintillator and photomultiplier to a known source of radiation.

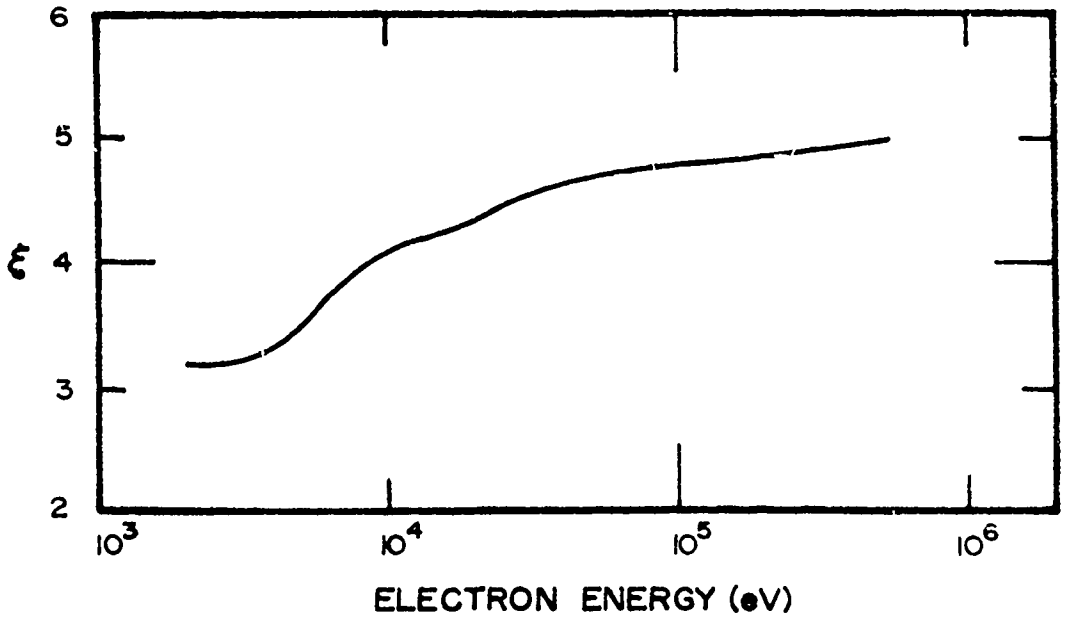

Figure 5. Energy dependent correction (ξ) of scintillator response for electron deposition.

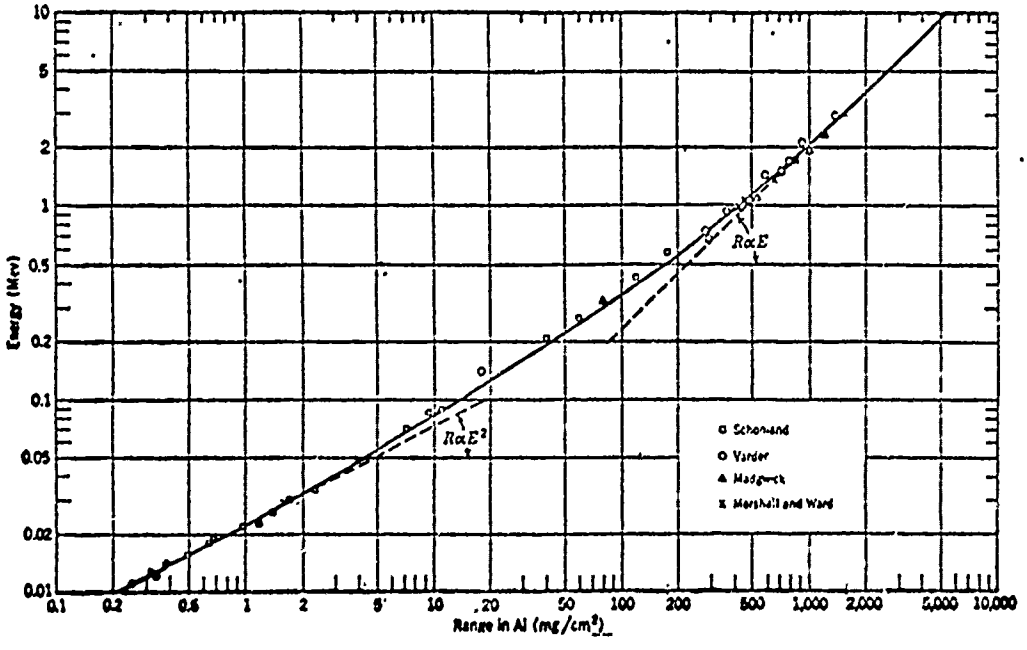

Figure 6. Critical energy range for electrons in aluminum. Taken from: L. Katz and A.S. Penfold, Revs. Mod. Phys., 24, 28(1952).

In this case, an Americium 241 source (5.5×10^6 ev alpha particles) is placed in contact with the calcium fluoride (europium activated) scintillator and the photomultiplier output current is measured at the normal photomultiplier operating voltage. The measured response for alpha particles is multiplied by ζ (Figure 5) to correct for the higher scintillator response to electron deposition [*Menifee*, 1966]. In calculating the energy dependence of ζ we have taken into account the average energy loss in the aluminum foil covering the scintillator.

Langmuir Probe

The Langmuir probe is used to measure the following ionospheric parameters:

1) Electron density
2) Electron temperature
3) Vehicle to plasma potential

The electron density measurement, however, is the primary measurement of this Langmuir probe model.

The instrument consists of an electrode (of known geometry) which is immersed in the ionospheric plasma, a function generator (which applies a voltage waveform to the electrode), and a logaritmic amplifier (which monitors the probe current flow). The desired parameters can then be calculated from a voltage-current curve such as the one shown in Figure 7 as follows:

1) Electron density is proportional to the electrode current in the electron accelerating region.

2) Electron temperature can be found from the expression describing the curve in the exponential part of the electron retarding region. The expression describing this region is:

$$i = I_o \exp \frac{eV}{kT}$$

where

V = negative electrode to plasma voltage

I_o = electron current when the electrode is at space potential (point of inflection)

e = electronic charge

k = Boltzmann's constant

T = electron temperature

By taking the logarithm of the above expression, electron temperature is found to be:

$$T = \frac{e}{K} \frac{V}{ln(i/I_o)}$$

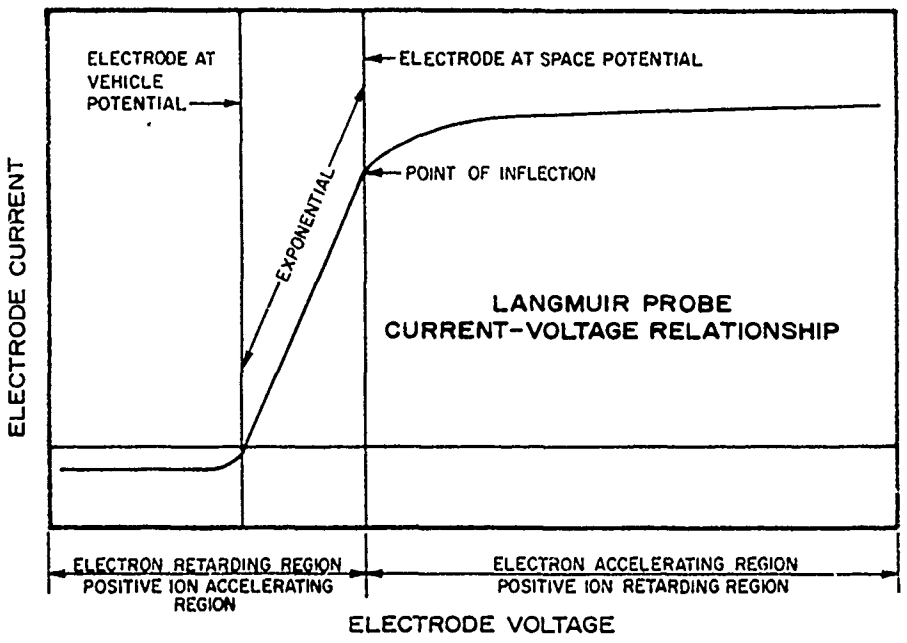

Figure 7. Langmuir probe characteristic voltage-current curve.

3) Vehicle to plasma potential is given by the voltage at the point of inflection in the voltage-current curve.

The spring loaded Langmuir probe electrode is mounted on a pivot and during ascent is held parallel to the length of the rocket by a door in the payload skin. When the rocket reaches altitude, the door ejects, allowing the electrode to pivot 90° so that it is perpendicular to the rocket major axis and is immersed in the ionospheric plasma.

The electrode consists of a guard electrode and a sensing electrode as shown in the block diagram of Figure 8. The electrode geometry is shown in Figure 9. Since the electrode currents are very small (10^{-9} to 5×10^{-5} amps), it is necessary to use a guard electrode to minimize displacement currents which flow as a result of the capacitance between the sensing electrode and the rocket. The guard electrode also minimizes field fringing effects on the end of the sensing electrode nearest the rocket and aids in defining electron density.

An improvement has been made in this Langmuir probe model by using a "clean electrode". The electrode is initially encased in a vacuum tight glass and metal container. It is then cleaned by baking for 24 hours at approximately 400°C and simultaneously pumping by a liquid nitrogen trapped diffusion pump. After the electrode has been vacuum baked, its container is backfilled with approximately 1 torr of argon gas and the electrode is cleaned even further using ion bombardment for one hour. The enclosure is then vacuum pumped and again backfilled to one torr pressure with pure argon gas. Container integrity and hence electrode cleanliness can easily be checked with a high voltage RF vacuum leak detector. During flight the glass envelope surrounding the electrode is fractured and discarded as the electrode extends into the plasma (see Figure 9).

A voltage waveform (Figure 10) is applied by the function generator to the guard electrode and one input terminal of the logarithmic amplifier (see Figure 8). If the current in the sensing electrode from the ionospheric plasma is zero, the voltages at A, B, C, and D (see block diagram) are forced to be equal to the function generator voltage. Since the voltages at C and D are equal, the output of the differential amplifier is zero. With a finite sensing electrode current, caused by electron attraction to the electrode, the voltages at C and D are not equal because the voltage at C is proportional to the log of the current into A, and $V_A = V_B = V_D$. The differential stage amplifies the difference giving an output proportional to the sensing electrode current.

The output from the differential amplifier is logarithmically compressed and may be either positive or negative. To make the signal compatible with the telemetry system, it is fed into the data splitter,

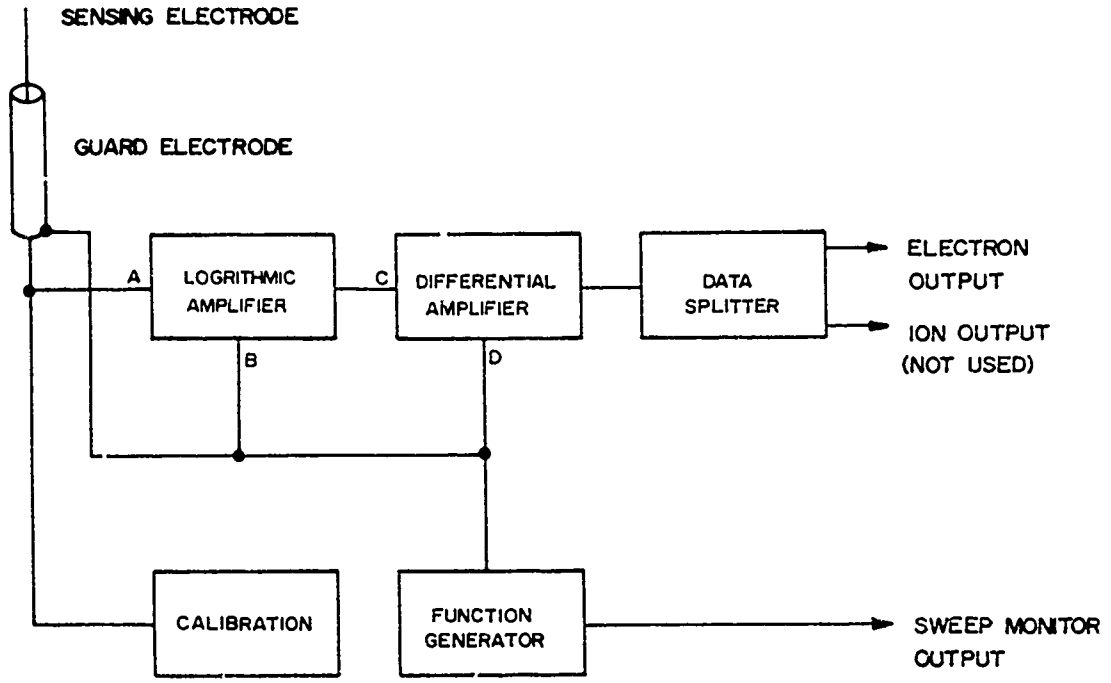

Figure 8. Langmuir probe block diagram.

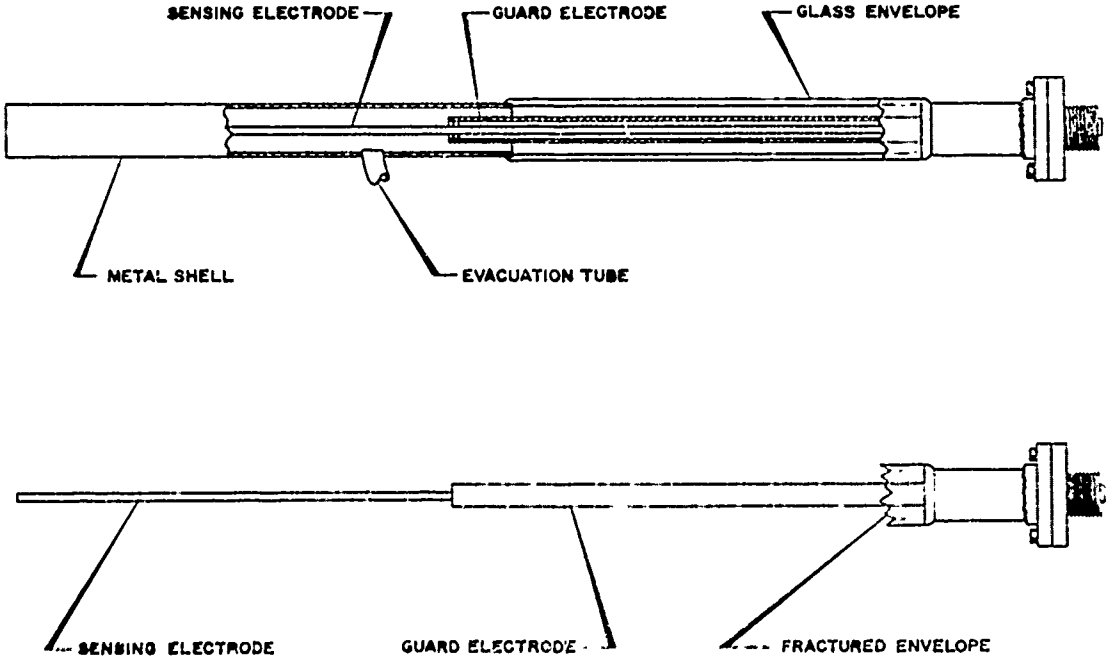

Figure 9. Langmuir probe electrode geometry.

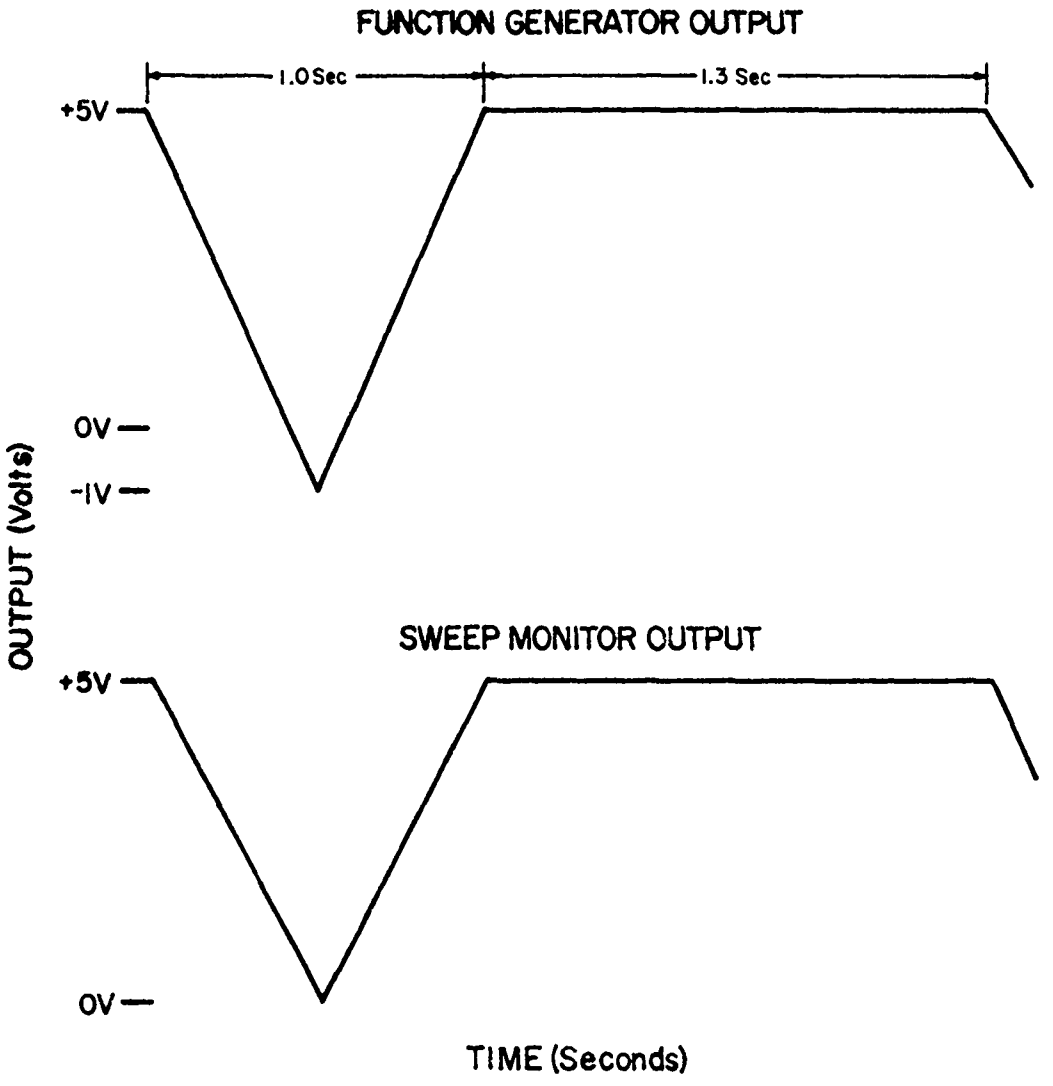

Figure 10. Langmuir probe function generator and sweep monitor waveforms.

which inverts one signal and provides two positive output signals. One output channel corresponds to positive ion current and the other to electron current (the output corresponding to ion current was not monitored on this flight). The data splitter in these models has been designed to clip off instrument response for values of electrode current less than 10^{-10} amps.

The calibration circuit provides a means of verifying instrument operation both during and prior to flight. This is accomplished by momentarily connecting a 1 megohm resistor from the instrument input to ground each 20 seconds for 25 ms. The output pulse magnitude depends on the sweep voltage at the time.

Retarding Potential Analyzer (HARP)

The HARP (Hyperbolic Analyzer of the Retarding Potential variety), developed by Hays and Sharp at the University of Michigan, is used to measure the differential energy spectrum of electrons with energies between approximately 1 and 500 ev. The instrument uses hyperbolic shaped plates swept in voltage to generate an axial retarding voltage and hence energy selection. Electrons within the acceptable energy range and within the field of view are counted by a channeltron. There are two sweep voltage ranges, 0 to 500 v and 0 to 50 volts which are alternately applied to the plates.

The field of view is determined by an aperture cut in a piece of foil located in the center of a 10" diameter ground plane. This field of view is centered approximately 15^{o} from the vertical axis of the rocket and has on the order of 1^{o} acceptance angle.

The ground plane which is forward of the remainder of the payload when the nose tip is removed is maintained at approximately 2.0 volts positive with respect to the rocket to insure that the electron retarding effects of a negative vehicle potential are overcome. A useful side effect of the biased ground plane is that when the sweep voltage is equal to or less than the ground plane voltage less the vehicle potential, electrons are accelerated through the aperture and are counted producing very high count rates. This rapid increase in count rate provides a measure of vehicle potential accurate to within a few millivolts.

The HARP has two data outputs. One is a monitor of the high voltage sweep and the second is a 16 segment hybrid commutator output multiplexed between analog and digital information. Both of these outputs are further described in the calibration section of this report. Table 4 lists the instrument specifications.

TABLE 4

HARP SPECIFICATIONS

Parameter	Value
Energy ranges	0-500 ev 0-50 ev
Energy resolution	10% FWHM
Field of view	1^{o} full angle
Geometric factor	9.2×10^{-4} cm^2 sr

3914 A Photometer

The photometer was included in the E-field payload to measure emissions from N_2^+ at 3914A. It viewed directly forward as illustrated in Figure 2. The specifications for this instrument are listed in Table 5.

TABLE 5

3914 A PHOTOMETER SPECIFICATIONS

Parameter	Value
Field of view	6^{o} full angle
Filter center wavelength	3915.6 A
Filter bandpass	15 A
Peak filter transmission	23%
Detectable signal range	.2 - 50 kR
PM tube type	4516 (RCA)

Figure 11 is a block diagram of the photometer. The photometer consists of a removable optical section, a miniature RCA phototube detector with its associated high voltage power supply, and a variable gain amplifier. The variable gain amplifier has a different gain for

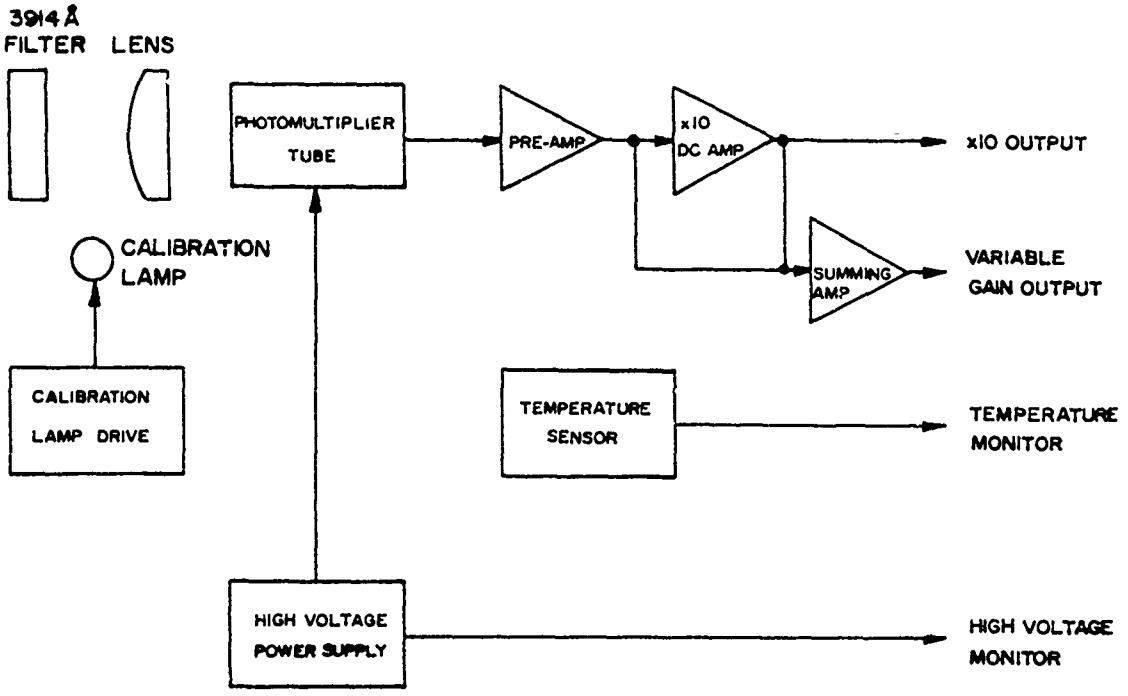

Figure 11. 3914 A photometer block diagram.

each of two input ranges. The gain at small signal levels is ten times the gain at large signals, thus extending the range of the instrument. The photometer also contains a light emitting diode which is turned on for 0.1 seconds every 30 seconds to provide a qualatative check on the operation of the instrument. This results in an output pulse 3.2 volts high. A temperature sensor circuit is used to monitor conditions near the photocathode of the detector tube.

Plasma Frequency Probe

The plasma frequency probe measures electron density and temperature in the E- and F-regions of the ionosphere. It directly measures the series and parallel resonant frequencies of an electrically short, RF excited antenna immersed in the ionospheric plasma. These measurements can then be converted to equivalent electron density and temperature and, when correlated with altitude, can provide an absolute electron density profile.

Basically, the plasma frequency probe operates by applying a sweeping RF signal (12 MHz to 1 MHz) to an antenna and monitoring the antenna current and voltage relationship. During alternate

frequency sweeps, the sweep is stopped at the series and parallel resonant points and the frequency is measured by a digital counter.

Figure 12 is a block diagram of the plasma frequency probe. The RF frequency sweep to the antenna is controlled by a ramp function from the sweep generator and is initiated by a reset pulse from the clock. As the ramp increases, the output frequency sweeps from 12 MHz to 1 MHz. As can be seen from the block diagram, an antenna current indication and a phase reference current are each fed to separate mixer circuits.

The two mixers are also fed by a second frequency which is a sweeping RF signal whose frequency is exactly 200 kHz below the antenna frequency and the relative amplitude and phase angle are coherent with the antenna current and reference signal inputs to the mixers. By use of this superheterodyne technique, the following amplifiers, clippers, and phase detector are not required to be wideband systems. The 200 kHz intermediate frequency amplifiers and clippers are identical for each channel.

The outputs of the clippers are constant in amplitude but shift in their phase relationship as the resonant points are approached. The outputs of the clipper amplifiers are fed to a phase detector which provides an output that indicates the phase relationship. This phase relationship will cross the 0^{o} point twice during each sweep from 12 MHz to 1 MHz, one point corresponding to the parallel resonance and the second corresponding to the series resonance.

The output from the phase detector to the gate and hold circuit initiates a signal which is fed to the sweep generator and stops the sweep for a period of 1 ms when parallel resonance is reached. During the 1-ms period, a 1 kHz clock signal opens a gate allowing the RF frequency (now holding) to activate the frequency counter where it is counted (in binary) and stored in the parallel shift registers. At the end of the 1-ms period, the sweep continues until series resonance is reached (where the phase relationship crosses back thru 0^{o}). The sweep is disabled again for 1 msec, during which time the RF frequency is again counted and stored in the series shift registers. At the end of the 2nd 1 msec time period, the sweep continues until a reset pulse from the clock starts the sweep at 12 MHz again. The reset pulse from

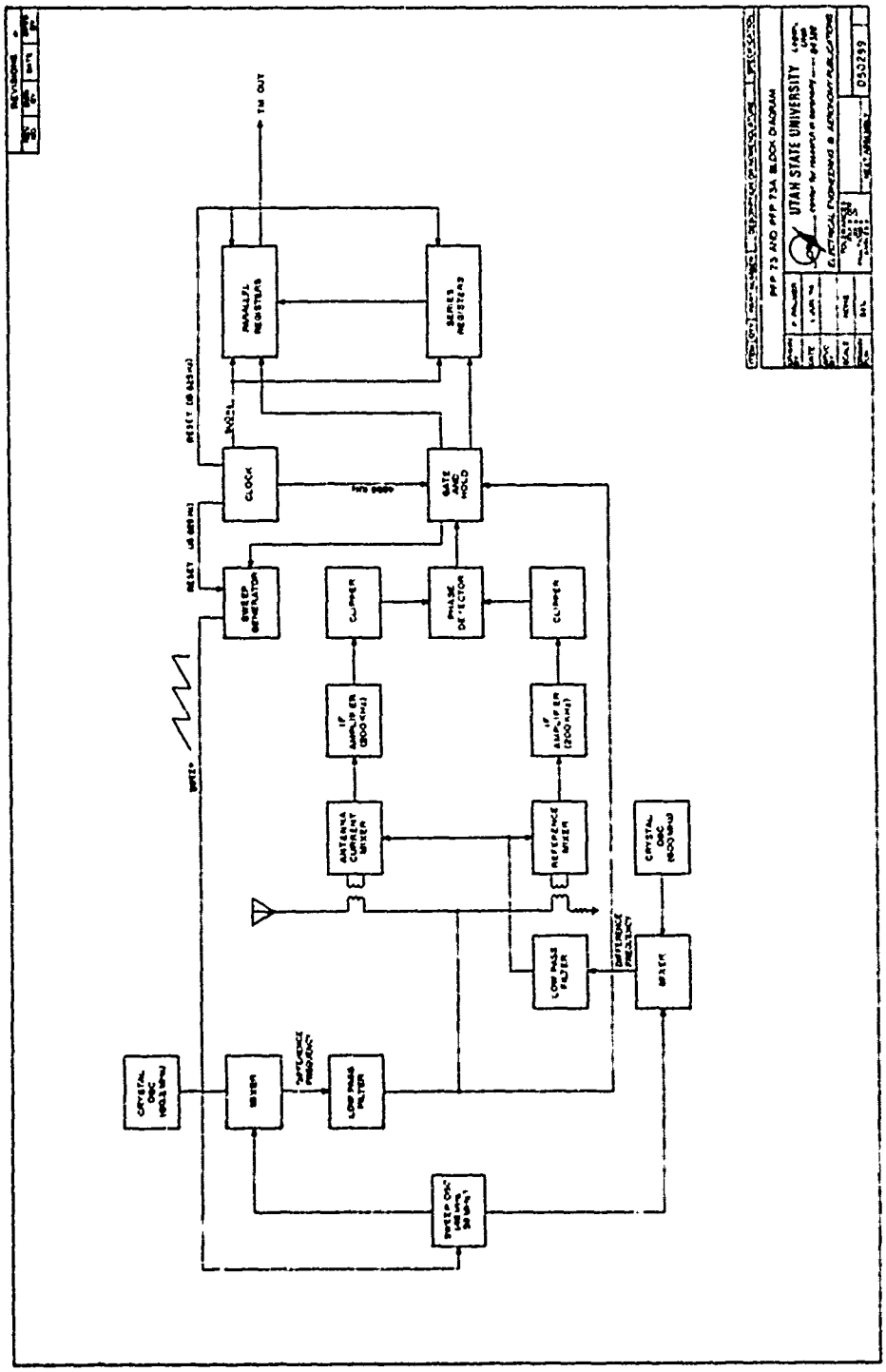

Figure 12. Plasma frequency probe block diagram.

the clock circuitry occurs at a frequency of 15.625 Hz, giving a total frame length of 64 ms. The information stored in the registers is telemetered out during the frame following the one in which it was stored, thus giving a delay of from 20-64 msec from the time it is obtained to the time it is telemetered.

Electron Spectrometer

The electron spectrometer measures electron spectra in the energy range from 100 to 1500 ev at count rates of 20 to 13,000 per second. Table 6 is a complete listing of the electron spectrometer specifications. Figure 13 is a block diagram of the instrument.

TABLE 6

ELECTRON SPECTROMETER SPECIFICATIONS (ES 73A-1)

Parameter	Value
Sweep range	366-24 volts
Sweep rate	1 per second
Energy range	100 to 1500 ev
Energy resolution	40% FWHM
Count rate	20 to 13,000 per second
Aperture radius	0.15 cm
Detector radius	0.15 cm
Separation distance	3.0 cm
Geometric factor	1.08×10^{-3} cm^2 ster
Field of view	8^o (full angle)
Channeltron serial number	2087009

As shown in the block diagram, electrons entering the instrument's aperture have their trajectories modified in an electric field created by applying a swept voltage across two curved parallel plates. To obtain the electric field, a positive voltage is applied to one plate and a negative voltage to the other. The potential difference is varied

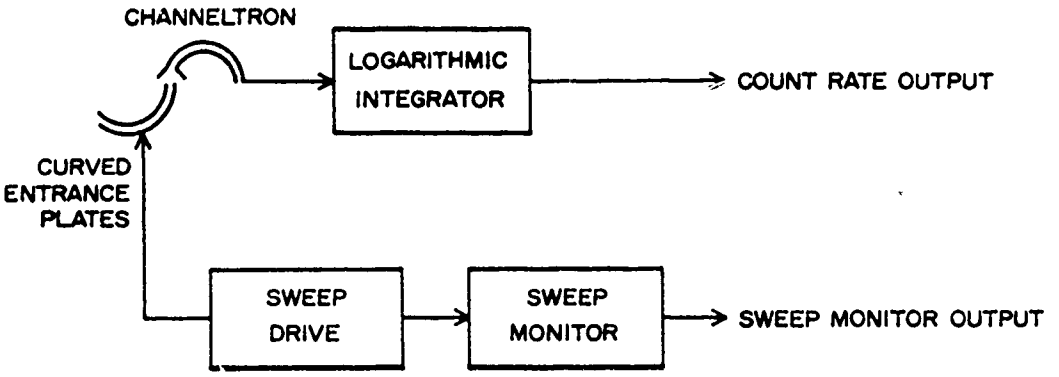

Figure 13. Electron spectrometer block diagram.

exponentially between 366 volts and 24 volts with a repetition time of 1 second. The plates are 5 mm apart, giving an electric field which varies between 73.2 kev/meter and 4.8 kev/meter. The electrons travel a distance of 3 cm between the plates. As the field strength is changed, electrons of various energies are detected by a channeltron detector placed at the end of the plates. To prevent the counting of low-energy thermal-electrons, a repelling screen with 82% transparency was placed in front of the entrance to the curved channel multiplier and a -15v potential was applied to the screen. A sweep monitor is provided which has an output voltage proportional to the energy of the electrons which are detected. The half power energy resolution is 40% at any given point on the sweep. The detector provides an output pulse for each electron that enters the aperture. These output pulses are fed into an amplifier to produce an output voltage that is approximately logaritmicaly related to the input count rate.

Particle Counter

The particle counter is designed to provide flux density and low resolution energy measurements of energetic electrons within a predetermined field of view. It has six detectors viewing in a common direction, and measures the number of electrons entering each detector.

Each detector responds to a different minimum energy level through the use of entrance windows of varying thickness. Specifications for the particle counter are shown in Table 7.

TABLE 7

PARTICLE COUNTER SPECIFICATIONS (PC 72B-4)

Channel	Half Power Energy Level (Kev) (Protons/Electrons)	Detector Type*	Detector S/N	Geometric Factor (cm^2 sr)	Half Angle Field of View	Window Type	Window Thickness/cm^2
1	25/4.5	CCM 4010C	None	$.335 \times 10^{-5}$	.682°	Poly-propylene (Sigmatron)	74 $\mu gm/cm^2$
2	70/9.0	CCM 4010C	None	$.112 \times 10^{-4}$	1.22°	Poly-propylene (Sigmatron)	156 $\mu gm/cm^2$
3	200/17.0	GM 705	28457	$.216 \times 10^{-2}$	7.44°	Mica	.35 mg/cm^2
4	400/28.0	GM 705	213453	$.509 \times 10^{-2}$	11.4°	Mica	.75 mg/cm^2
5	650/42.0	GM 711	211105	$.622 \times 10^{-1}$	9.58°	Mica	1.8 mg/cm^2
6	1100/86.0	GM 711	17733	.296	21.05°	Mica plus aluminum	1.8 mg/cm^2 (Mica) 4.8 mg/cm^2 (Al)

*CCM's are Bendix, GM's are LMD

Figure 14 is a block diagram of the particle counter. Channeltrons are used as detectors for the two low energy channels and geiger tubes are used as detectors in the four high energy channels. The output pulses from the detectors are fed into logarithmic intergrators that provide analog voltages proportional to the log of the count rate in each channel. The analog outputs of the logarithmic integrators are fed into a 16 segment, 10 frames per second electronic commutator. The commutated signal is then sent to the rocket telemetry system.

Instrumentation for Support

Included in the PT10.312-3 payload was support instrumentation for payload despin, payload tracking, attitude determination, determination of magnetic pitch angle, data recovery and payload recovery. Technical data, where appropriate, are included in Appendix B.

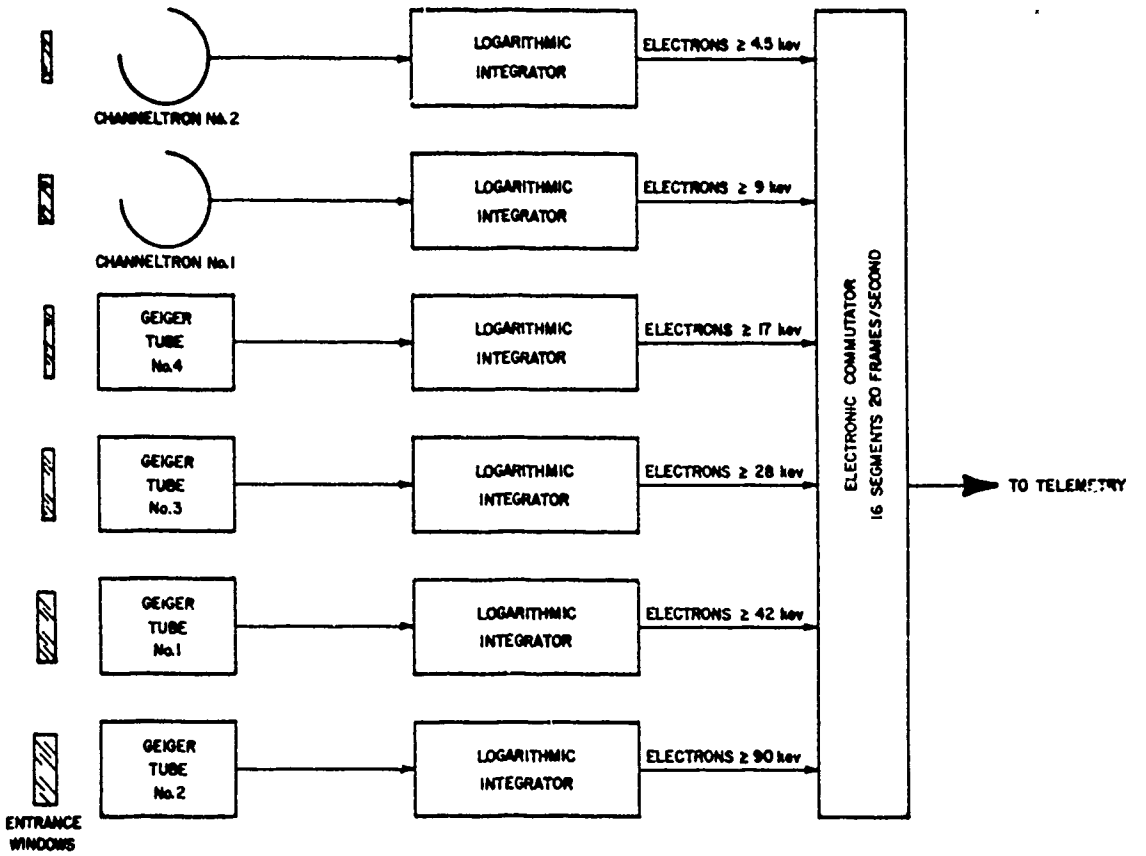

Figure 14. Particle counter block diagram.

GROUND SUPPORT MEASUREMENTS

Four groups performed ground based experiments and support measurements on the night of the Paiute Tomahawk launch. The purposes of the measurements were to determine launch criteria and to supply support data which to use as an aid in the analysis of the data accumulated by the rocketborne instruments. The support data includes the following:

1) The visible and IR optical measurements made by Utah State University (USU);
2) The Chatanika Radar electron density measurements made by Stanford Research Institute (SRI);
3) The optical, geomagnetic, photographic, and ionospheric measurements made by the University of Alaska;

4) The electron density measurements made by the Department of Commerce Office of Telecommunications (OT/ITS) partial reflection sounder.

Brief descriptions of each experiment and preliminary results are given in the following pages.

USU's Visible and IR Measurements

Utah State University operated photometers, radiometers, and interferometers at the Poker Flat Range on the night of the launch. A summary of the various instrument capabilities, purposes, and operations is given in Table 8. All of the instruments obtained information which will give useful inputs toward the detailed analysis of the rocket data. In addition, the photometers provided information for determining the intensity and location of an auroral arc which was necessary for launch.

The instruments were looking through scattered clouds during the launch period. All instruments were looking at 66° elevation and 24° true azimuth, which corresponded to the payload 100 km entry point, except the scanning photometers and the IR field widened interferometer. The photometers were scanning from horizon to horizon on a 24°/204° true azimuth, and the interferometer was looking at the zenith.

In addition to the data taken during the night of the launch, similar data were taken on several nights before and after the launch date.

Chatanika Radar Measurements

The Stanford Research Institute incoherent scatter radar system uses an 85 ft parabolic steerable antenna and a 4 megawatt Klystron Tube Transmitter to measure electron densities, electron and ion temperatures, plasma transport velocities and electric fields at altitudes between 70 km and several hundred km. The radar measurements were backed up with a 35 mm narrow field camera coaligned with the directional radar system.

On the night of the launch, the radar unit was operational from about 0815 to 0945 universal time. The elevation was set at 70 degrees

TABLE 8

CHARACTERISTICS AND SUMMARY OF USU'S GROUND INSTRUMENTATION FOR SUPPORT OF PT10.312-3 LAUNCH

Instrument	Wavelength Response	Resolution or 50% Bandwidth	FOV Full	Purpose of Measurement	Time Interval of Proper Operation
Scanning photometer	3914A optical filter	Approx. 4A	5°	Establish auroral arc location and intensity for launch criteria and support rocket analysis with airglow and auroral intensities, locations and forms.	0700 to 1000 UT.
Scanning photometer	6300A optical filter	Approx. 4A	5°		0700 to 1000 UT.
Scanning photometer	5577A optical filter	Approx. 4A	5°		0700 to 1000 UT.
Photometer	3914A optical filter	Approx. 4A	5°	Establish auroral intensities and support rocket data analysis.	0700 to 1000 UT.
Photometer	5577A optical filter	Approx. 4A	5°		0700 to 1000 UT.
Rocking filter photometer	4278A, 5575A, 6300A 5900A, 8350A variable with angle	Approx. 4A	5°	Support rocket data by measuring N_2^+, OI, H Beta, and OH.	Periodically operated for short times from sunset to 1000 UT.
IR Field Widened Interferometer (IR,FWI)	1.0μ to 1.5μ	4 cm^{-1}	6°	Determine spectral characteristics and intensities from 1 to 1.5μ in auroral and nonauroral conditions to further define auroral characteristics during and around the launch period.	0644 to 0934 UT.
Radiometer	1.700 fixed	.0773	10°	Support rocket data by measuring OH(5,3)	0700 to 1000 UT.
Radiometer	1.574 fixed	.212	10°	Support rocket data by measuring OH, N_2^+, & N_2.	0700 to 1000 UT.
Radiometer	1.53 fixed	.0-	10°	Support rocket data by measuring N_2^+.	0700 to 1000 UT.
Radiometer	1.703 fixed	.0773	1.8°	Support (IRFWI) measurements.	0700 to 1000 UT.
Radiometer	1.27 fixed	.0254	10°	Measure $O_2(^1\Delta)_{00}$ band intensity.	0700 to 1000 UT.
Radiometer (cold)	1.685 & 2.192	.0773 ;.176	7°	Support rocket data by measuring OH(9.7) and OH(5,3).	0800 to 0900 UT.
Visible Field Widened Interferometer.	7400A to 9000A	6 cm^{-1}	10°	Provide spectra support data for temperature measurements and rocket data analysis.	0830 to 1000 UT.

and the azimuth was in a scanning mode until a short time before the launch. Shortly before the launch the radar antenna was switched to an azimuth and elevation which looked directly at the lower portion of the auroral arc of interest. After about 15 minutes in this position, it was returned to its previous scanning mode. No operational problems of any significance were encountered.

The measurements indicated that there was activity which corresponded with the launch criteria which required a stable auroral arc. Data were routinely taken on other nights during the ICECAP program. All of the data are being reduced in a routine manner and will be available on request from SRI.

University of Alaska Measurements

The University of Alaska had riometers, magnetometers, cameras, photometers, and an ionosonde operating at various locations on the night of the launch. These instruments and their locations are listed in Table 9. The data from the photometers, riometers, and magnetometers were used to determine the launch conditions. Specifically, the scanning photometers from Ester Dome and Fort Yukon were used to determine the position and intensity of the auroral arc which the rocket was fired over. All of the data from the instruments should be useful for correlation with the rocket data.

Office of Telecommunications (OT/ITS) Partial Reflection Experiment

OT/ITS operated a 2.2 and 9 megahertz transmitter and receiver system to determine electron densities at various altitudes. The unit is located at Poker Flat, and takes measurements in the zenith direction. It operates by measuring the parital reflection of the transmitted signal off of the ionosphere. Detailed information on its operation during and around the launch have not been made available as of the writing date of this publication. However, the unit was operational at various times throughout the ICECAP program.

TABLE 9

UNIVERSITY OF ALASKA GROUND INSTURMENTATION FOR

SUPPORT OF PT10.312-3 LAUNCH

Instrument	Location	Description
All Sky Camera	Ester Dome (College), Chatanika, Fort Yukon	16mm & 35mm black & white photographs with 100° FOV, one 10 sec exposure is made per minute to T-10 min; continuous coverage from T-10 min to T+10 min.
Riometer	Poker Flat, Fort Yukon Ester Dome (College)	Measures ionospheric absorption of 30 megahertz galactic radio noise.
Magnetometer	Poker Flat, Fort Yukon Ester Dome (College)	Three component magnetometer for measuring disturbances in the geomagnetic field. The college station has storm and rapid run magnetograms available.
Ionosonde	College	Measures peak electron density overhead, swept frequencies .5 to 20 MHz, normal incidence.
Meridian Scanning Photometers	Ester Dome, Fort Yukon	Measures auroral intensity at 5577A, 3914A, 6300A, and 4861A along the meridian path.

RESULTS

Paiute Tomahawk 10.312-3 was launched from Pad 1 of the Poker Flat Research Range, Alaska, on 18 April 1974 at 0804:15.201 GMT. The payload had been on the launch rail for 11 days before proper launch conditions developed. All payload monitors and instrument outputs indicated a completely functional payload before launch. Proper staging of the booster and sustainer rocket motors occurred and the payload flew over a stable auroral arc obtaining an apogee of 185 km. Data were obtained from seven of the eight payload experiments (high voltage failure occurred in the soft electron spectrometer). The recovery sequence occurred at the designated times and the payload was recovered during early morning on the day following the launch.

The NASA VERLORT radar obtained a good track of the payload from the on-board S-band beacon. Figures 14 and 15 show the PT10.312-3 trajectory. The telemetry signal received during the flight was strong and data were good for all but a short time. During that interval some of the data channels exhibited noise. The problem terminated abruptly, however, and the data channels were then clean for the remainder of the flight.

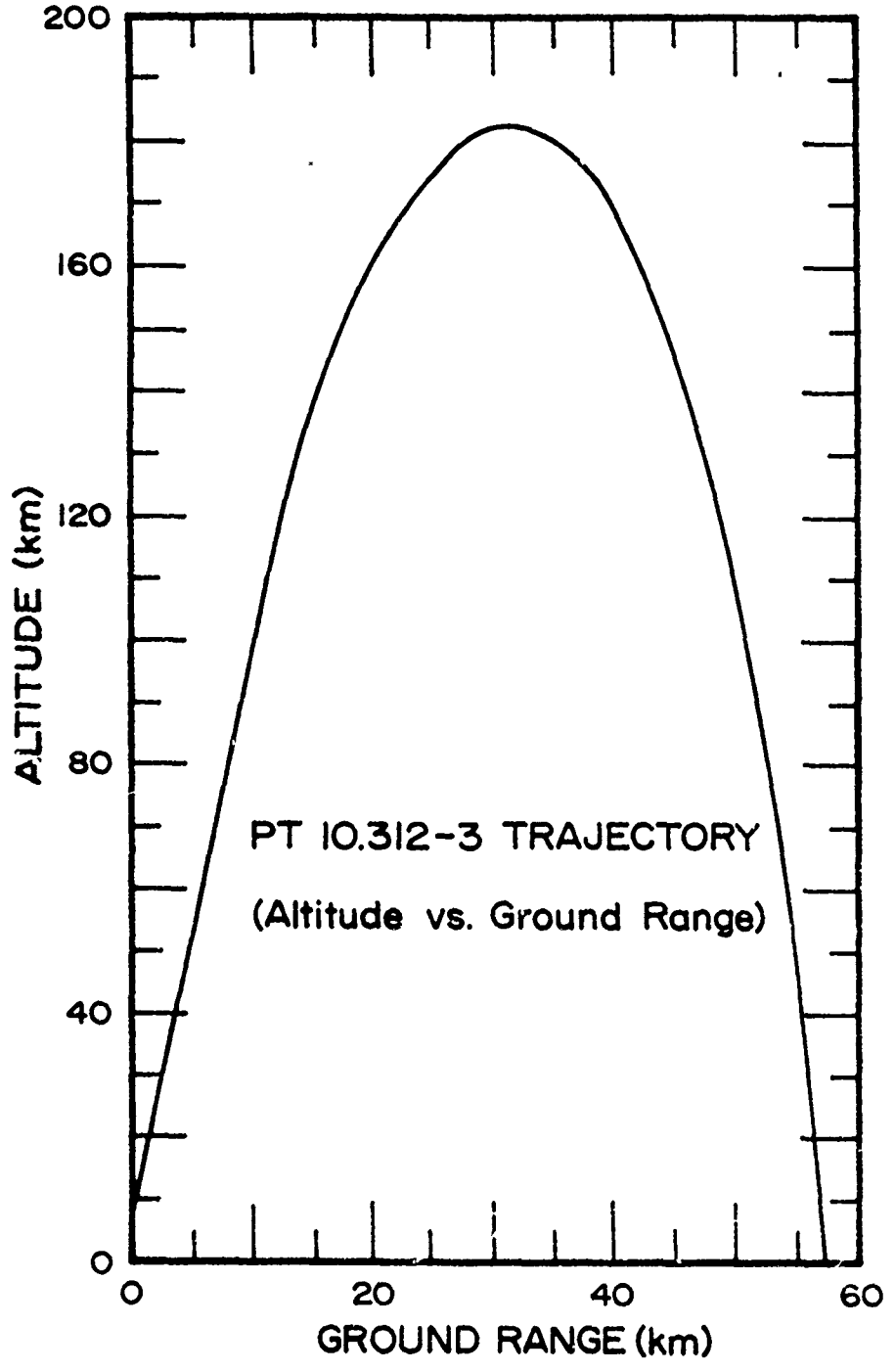

Figure 15. PT10.312-3 trajectory - altitude vs. ground range.

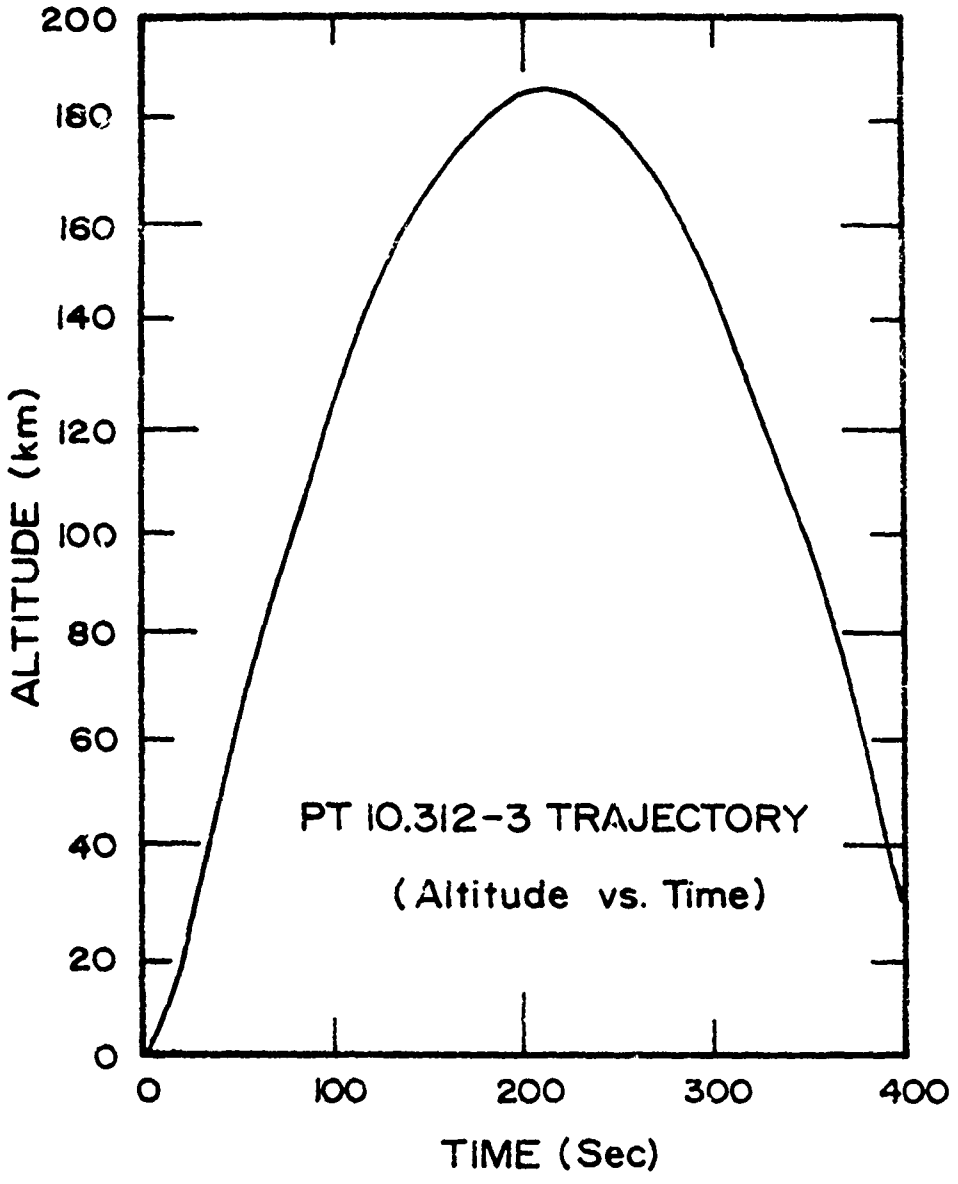

Figure 16. PT10.312-3 trajectory - altitude vs. time from launch.

REFERENCES

Burt, D.A. and C.D. Davis, Rocket instrumentation for ICECAP 73A auroral measurements program -- Black Brant 18.205-1, *Scientific Report No. 3, HAES Report No. 3, AFCRL-TR-74-0195,* 147 pp., Contract F19628-72-C-0255, Space Science Laboratory, Utah State University, Logan, February 1974.

Maynard, N.C., Electric fields in the ionosphere and magnetosphere, in *Magnetosphere-Ionosphere Interactions,* edited by K. Folkstead, p. 155, Universitetsforlaget, Oslo, 1972.

Menefee, J., C.F. Swineheart, and E.W. O'Dell, Calcium Fluoride as an x-ray and charged particle detector, *IEEE Trans. Nucl. Sci., NS-13,* 720, 1966.

Sternglass, E.J., Backscattering of Kilovolt Electrons from Solids, *Phys. Rev., 95,* 345, 1954.

APPENDIX A

INSTRUMENT TECHNICAL DATA

TABLE A-1

E-FIELD PROBE 10x30 COMMUTATOR ASSIGNMENTS

Pin No.	Function
1	2.5V
2	DC x 10
3	Antenna extension mon.
4	+15V mon.
5	-15V mon.
6	DC x 1/4+
7	DC x 1/4-
8	DC x 10
9	DC x 2
10	Filter #1 20-70 Hz
11	Filter #2 100-300 Hz
12	Filter #3 300-500 Hz
13	Filter #4 500-1000 Hz
14	DC x 10
15	Filter #5 1000-3000 Hz
16	Filter #6 10^4 - 10^5 Hz
17	DC x $1/4^+$
18	DC x $1/4^-$
19	DC x 2
20	DC x 10
21	Filter #1
22	Filter #2
23	Filter #3
24	Filter #4
25	Filter #5
26	Filter #6
27	Ov
28	+5V
29	+5V
30	+5V

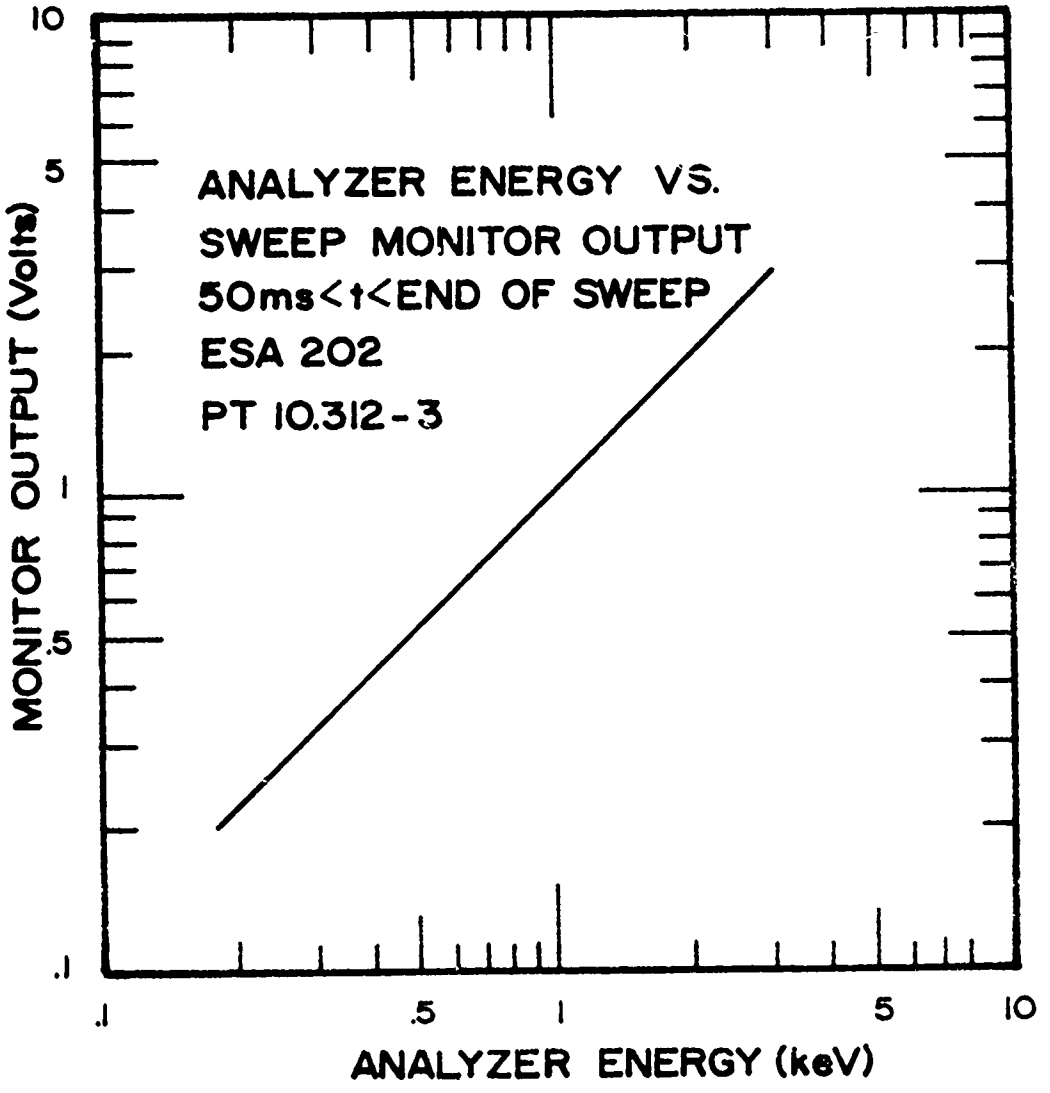

Figure A-1. Analyzer energy vs. sweep monitor output ($V_{sweep} = .96 \times 10^{3} V_{sweep\ monitor}$). The monitor voltage rise time is slower than the sweep voltage rise time. For this reason, the monitor voltage should not be used for calibration for times less than 50 milliseconds after the start of the sweep. The calibration data for times less than 50 milliseconds after the start of the analyzer voltage sweep are given in Figure A-2. Electron energy versus sweep time for times greater than 50 milliseconds is given in Figure A-3.

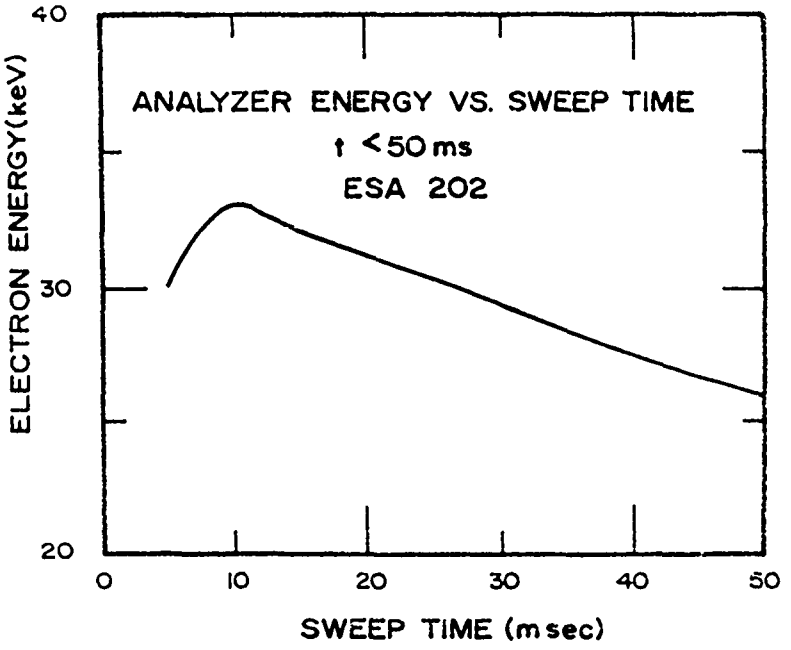

Figure A-2. Analyzer energy vs. sweep time for t < 50 ms.

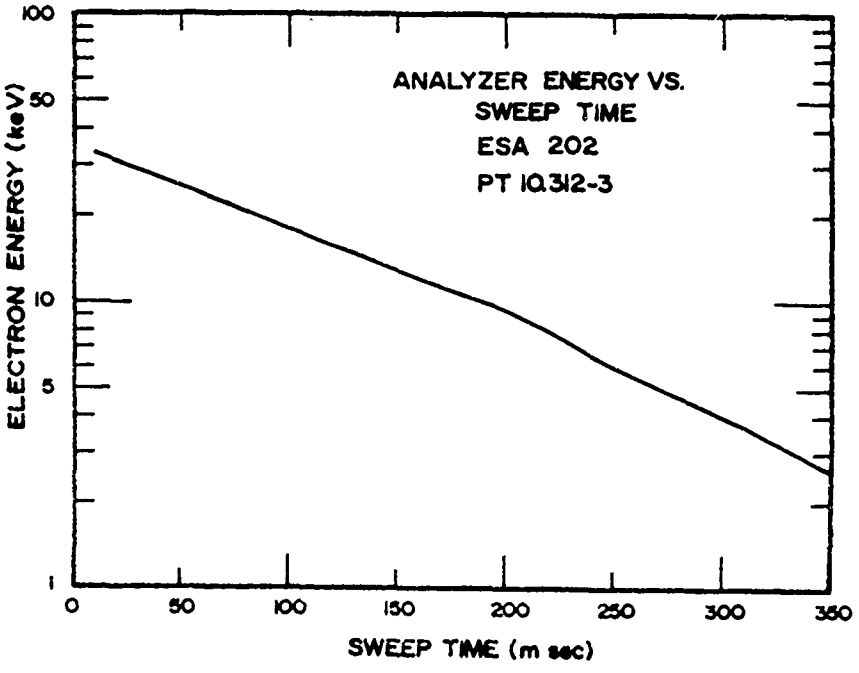

Figure A-3. Analyzer energy vs. sweep time for t > 50 ms.

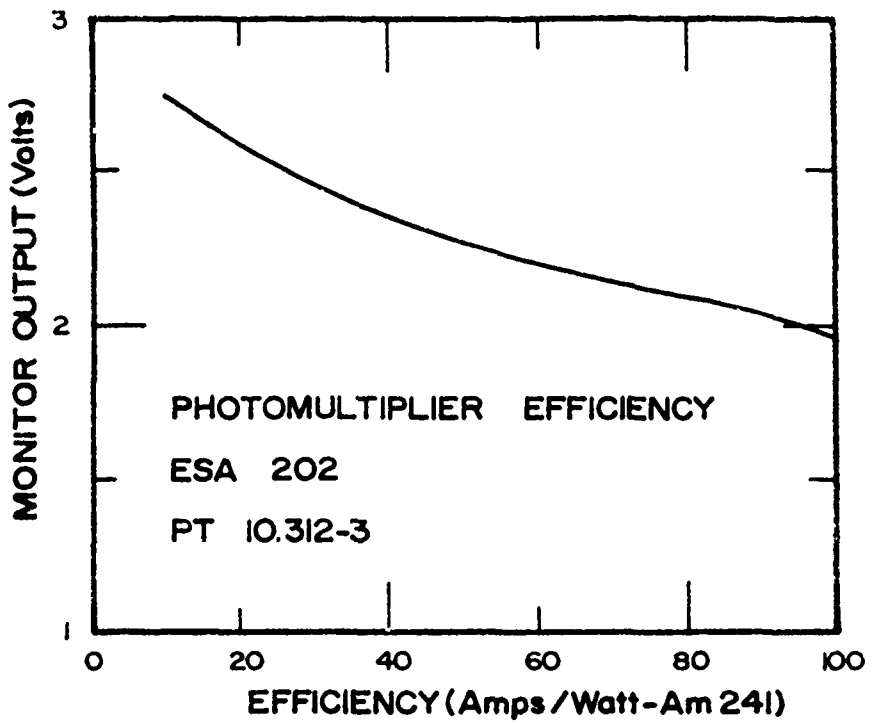

Figure A-4. ESA photomultiplier effeciency.

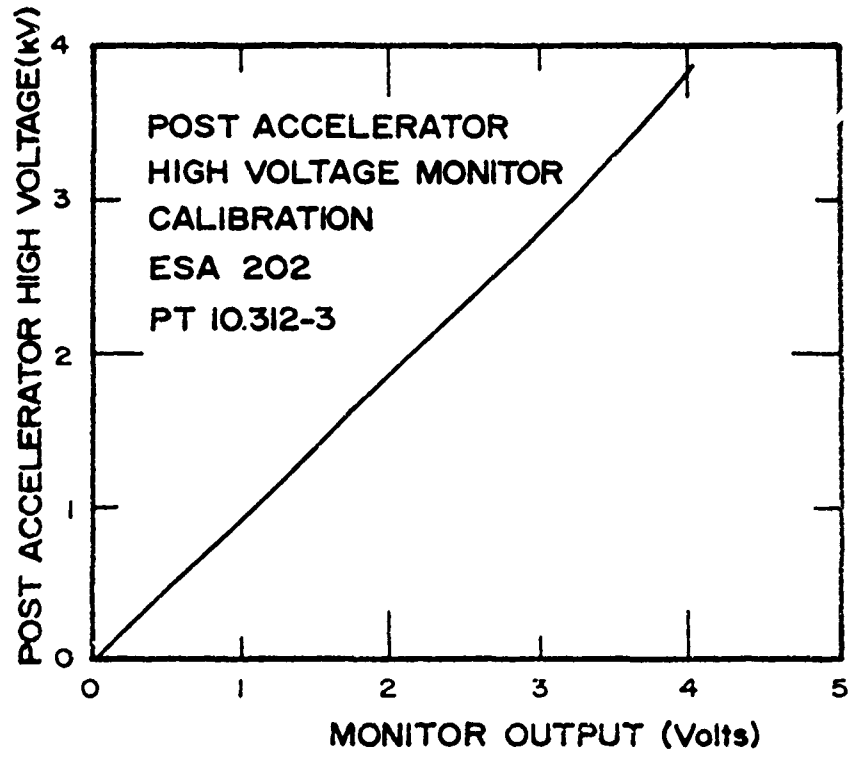

Figure A-5. ESA post accelerator high voltage monitor calibration.

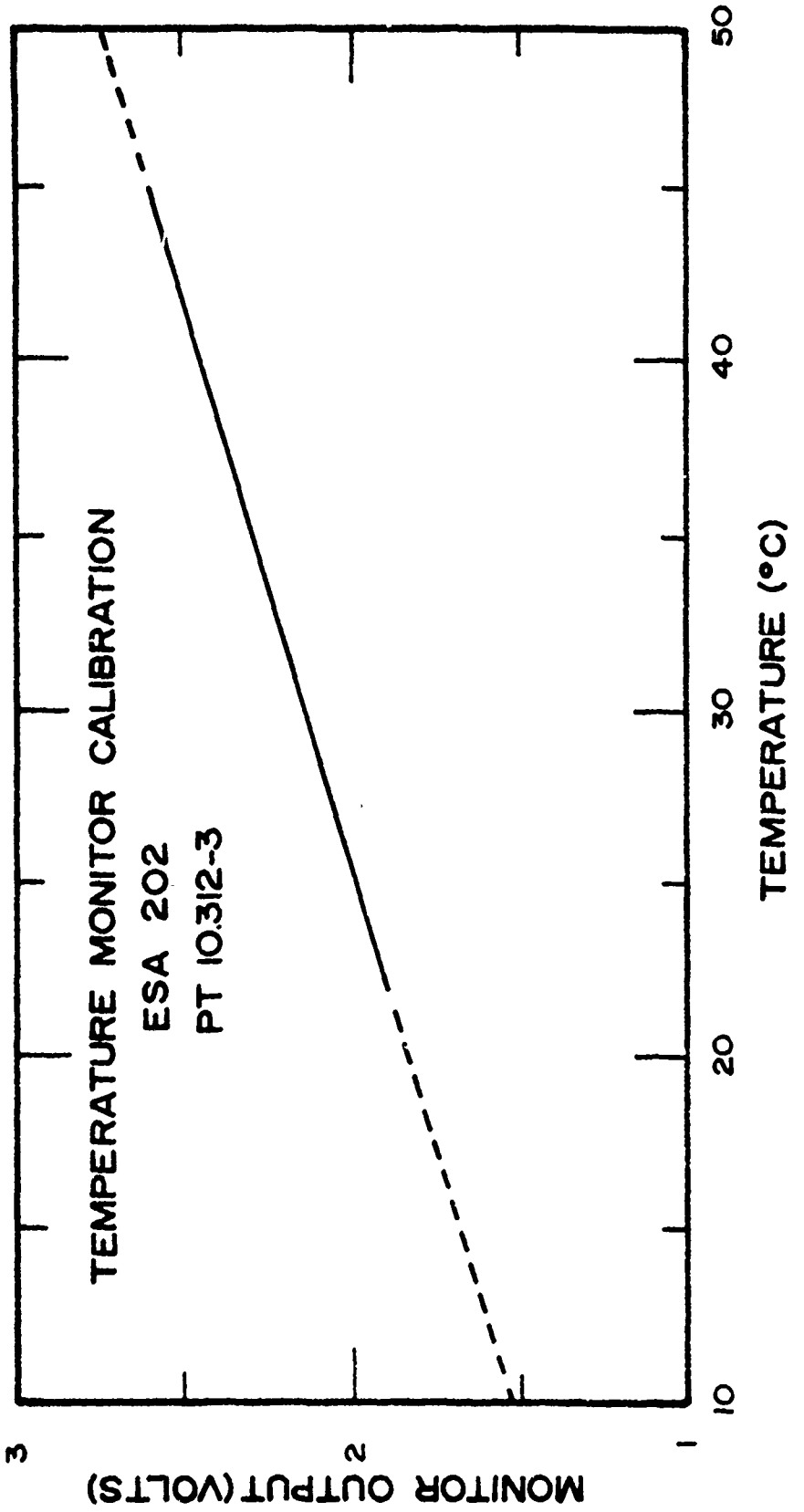

Figure A-6. ESA temperature monitor calibration.

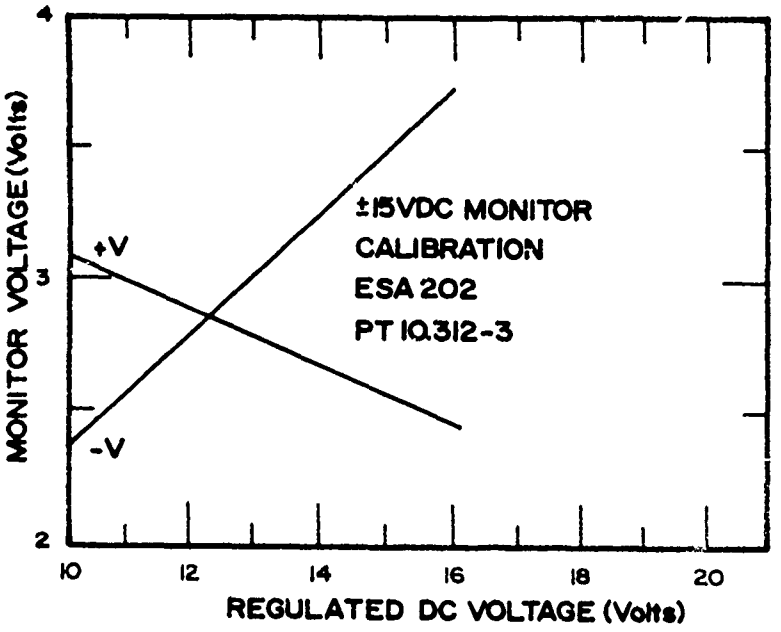

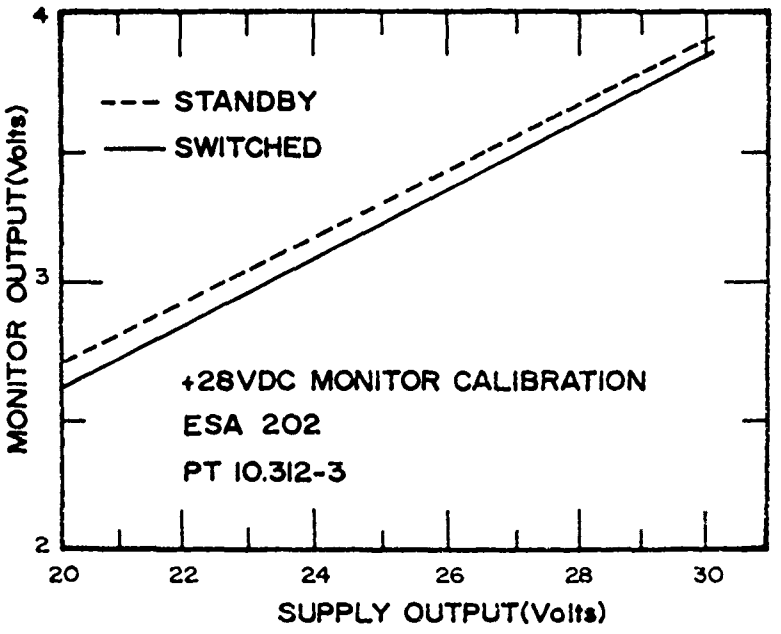

Figure A-7. ESA power monitor calibrations. A cover monitor was also provided with a .60 volt output with the cover on and a 4.67 volt output with the cover off.

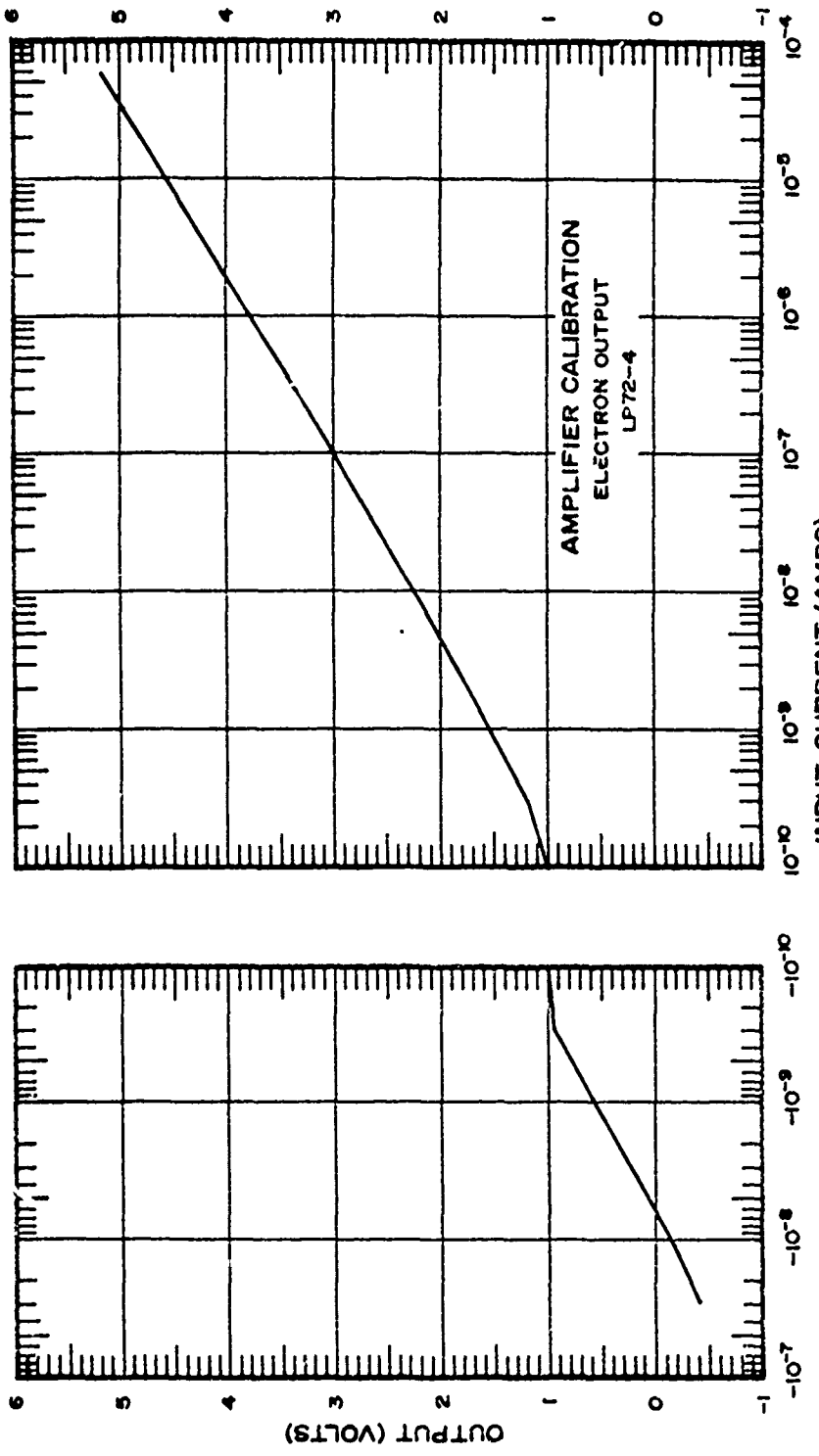

Figure A-8. LP 72-4 amplifier calibration - electron output.

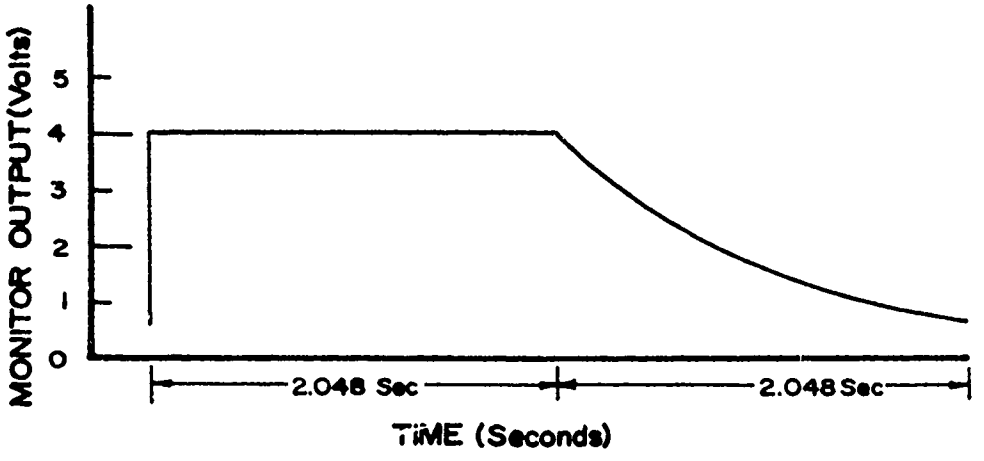

Figure A-9. HARP sweep monitor waveform.

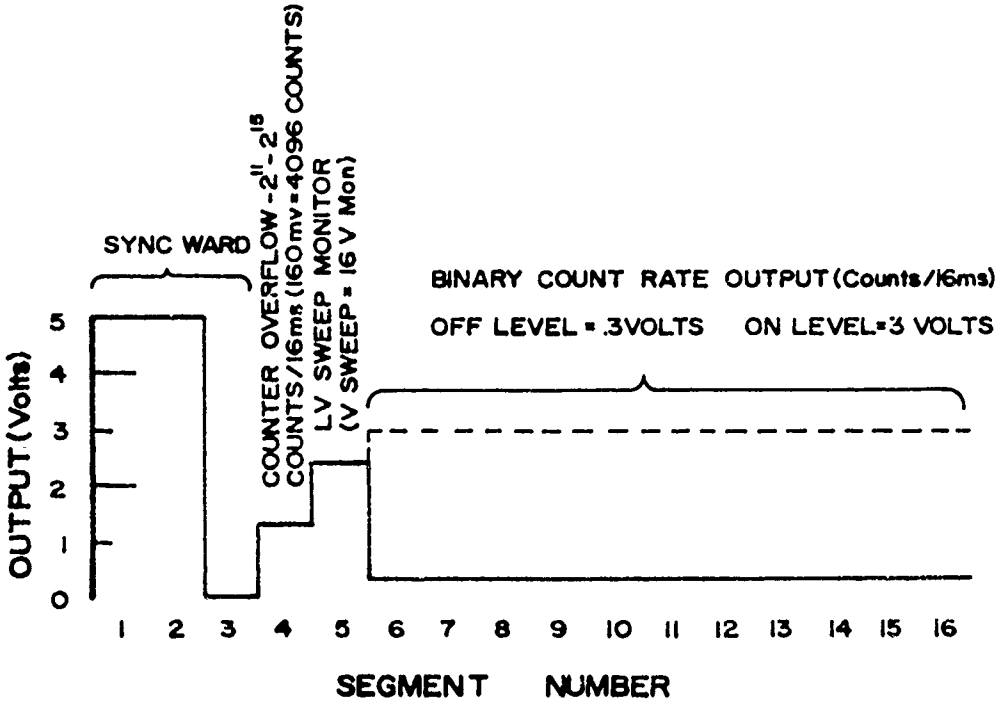

Figure A-10. HARP commutator output data format.

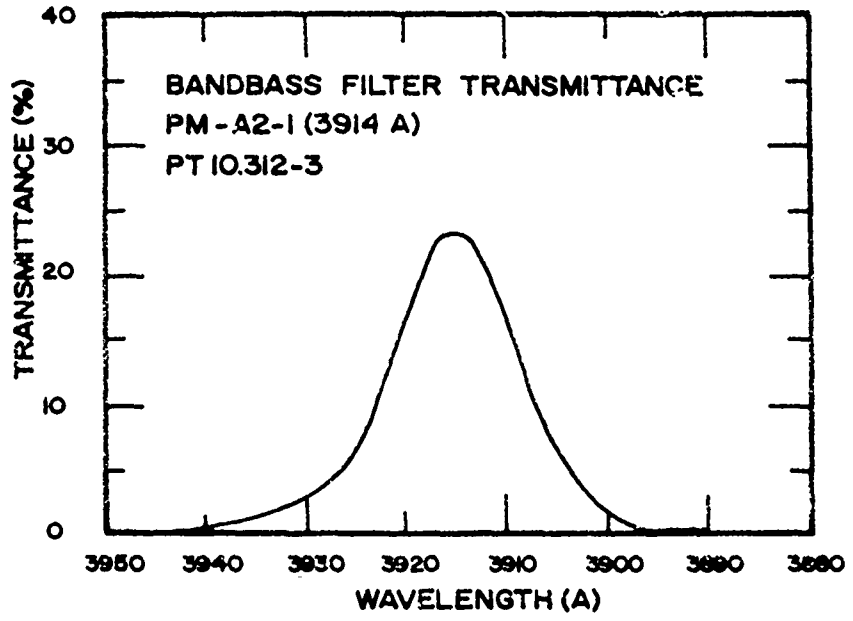

Figure A-11. 3914 A photometer bandpass filter transmittance.

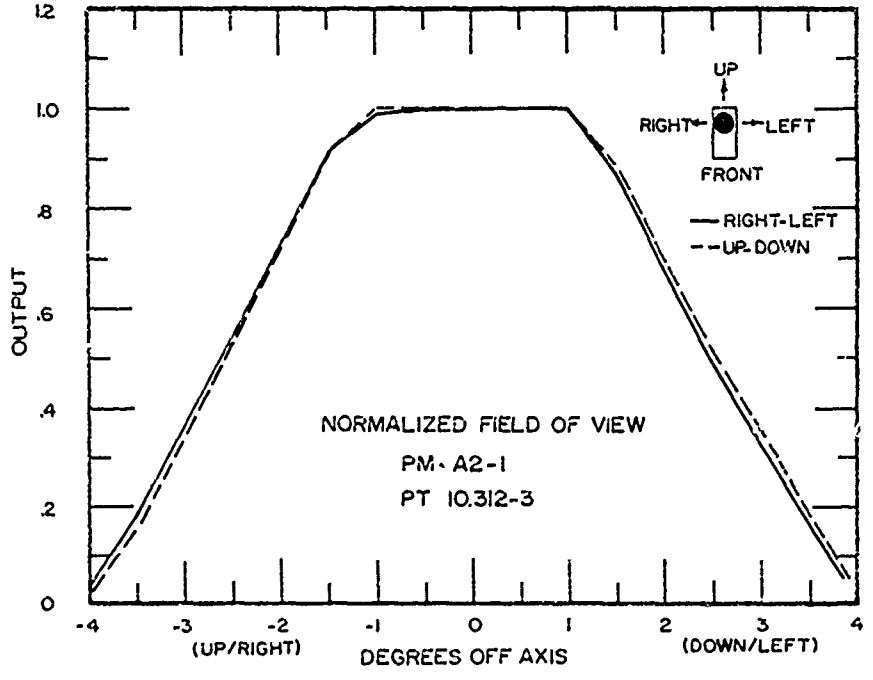

Figure A-12. 3914 A photometer field of view.

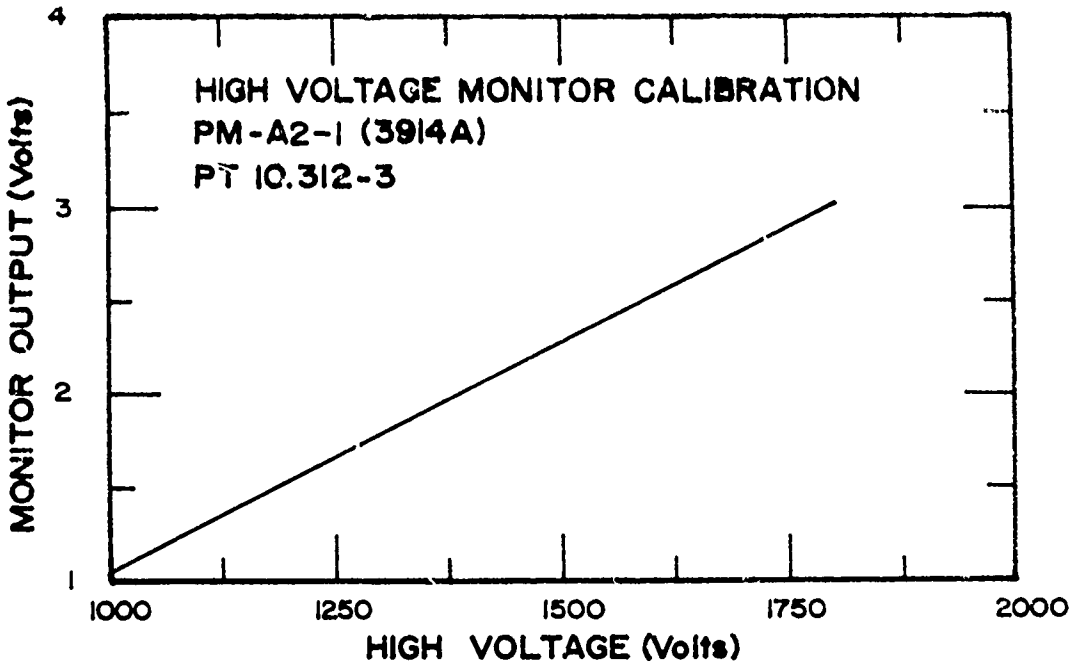

Figure A-13. 3914 A photometer high voltage monitor calibration.

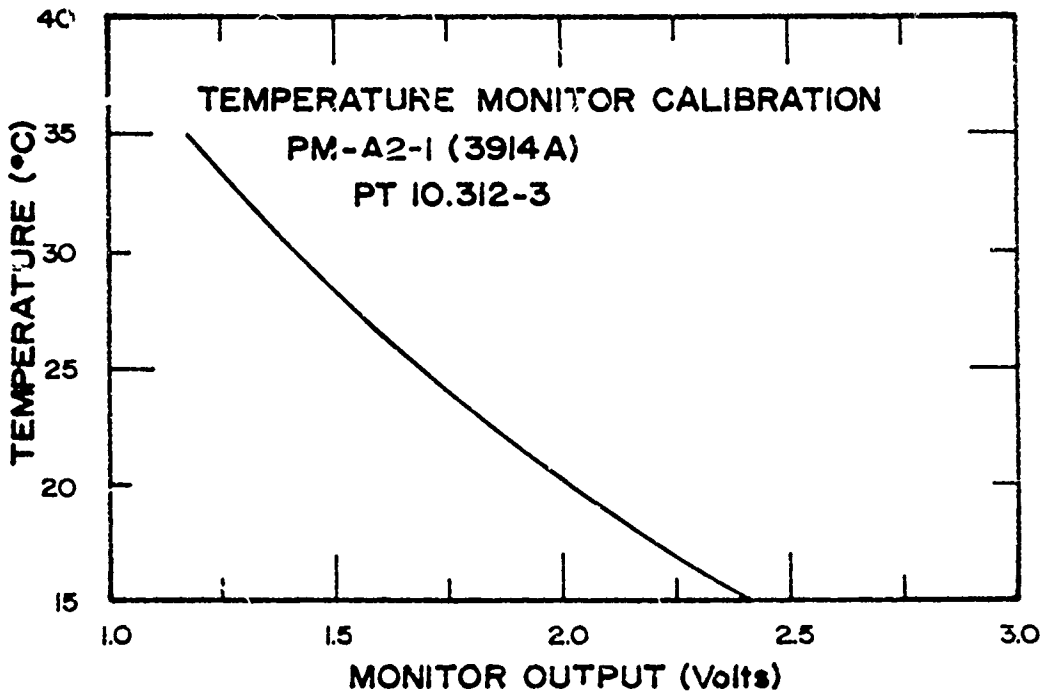

Figure A-14. 3914 A photometer temperature monitor calibration.

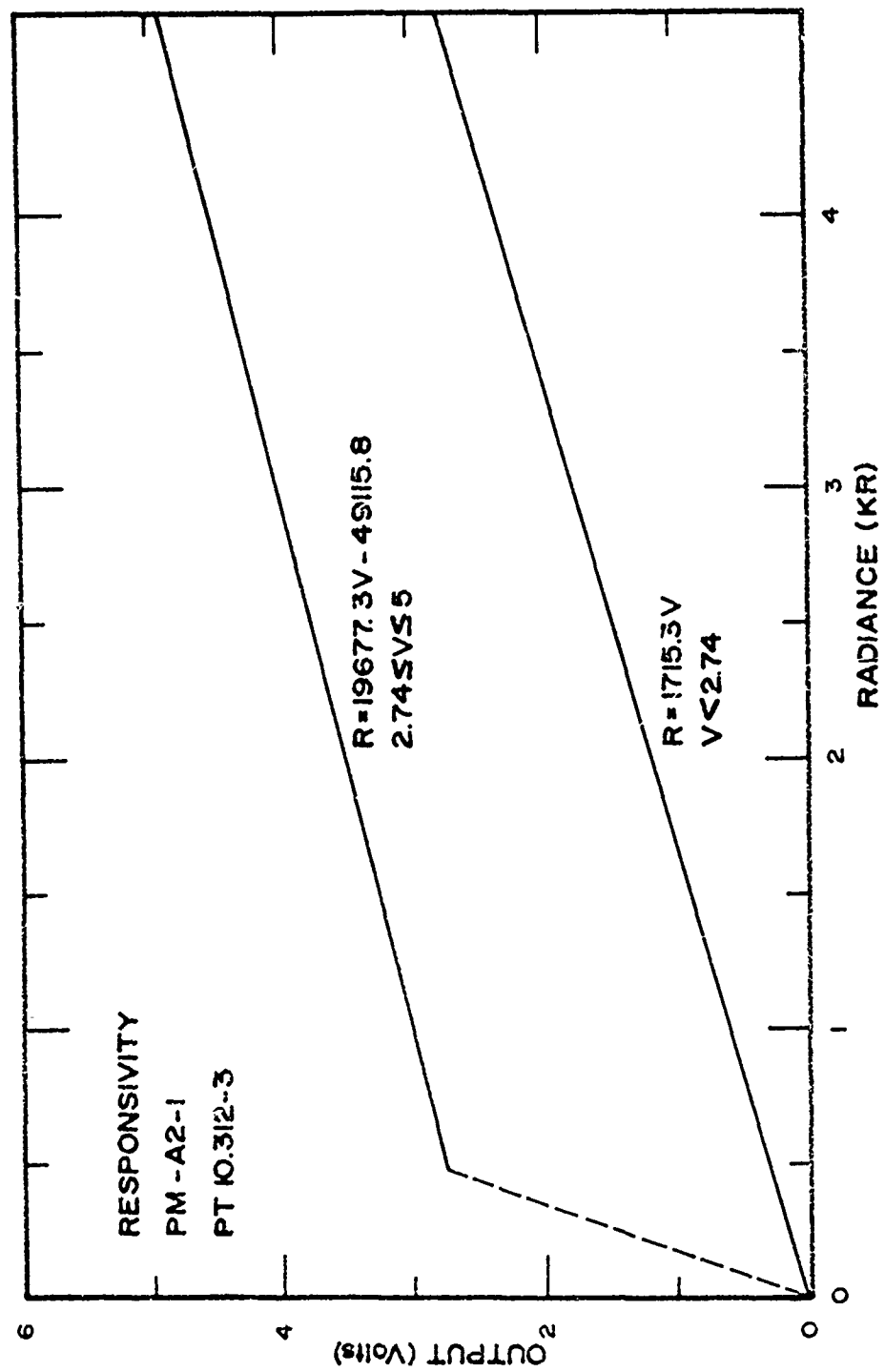

Figure A-15. 3914 A photometer responsivity.

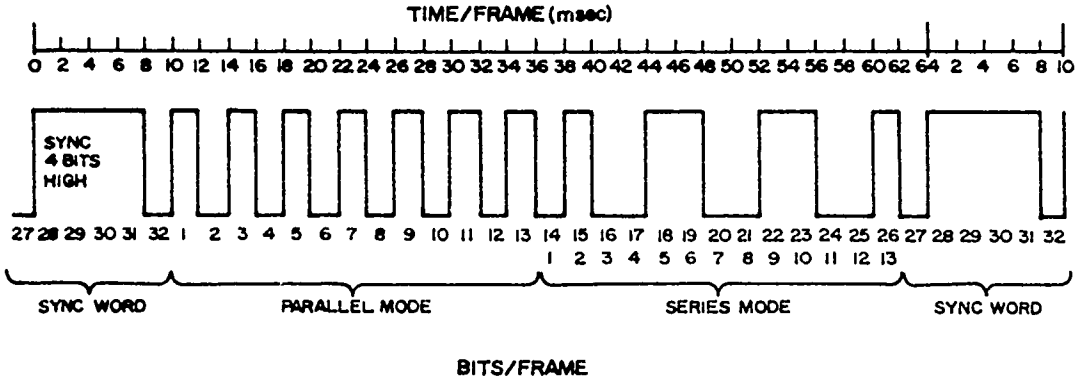

Figure A-16. Plasma frequency probe output data format.

TABLE A-2

PLASMA FREQUENCY PROBE DATA OUTPUT FORMAT FOR FREQUENCY DETERMINATION

Bit No.	Frequency Indicated by Positive Output (kHz)
1	8192
2	4096
3	2048
4	1024
5	512
6	256
7	128
8	64
9	32
10	16
11	8
12	4
13	2
14	

Note: $T_{res} = T_{csb} + T_{f/s}$

where

T_{res} = Time of resonance

T_{csb} = Time of center of sync word of previous frame

$T_{f/s}$ = Time after reset at which resonance occurs (see Figure A-17).

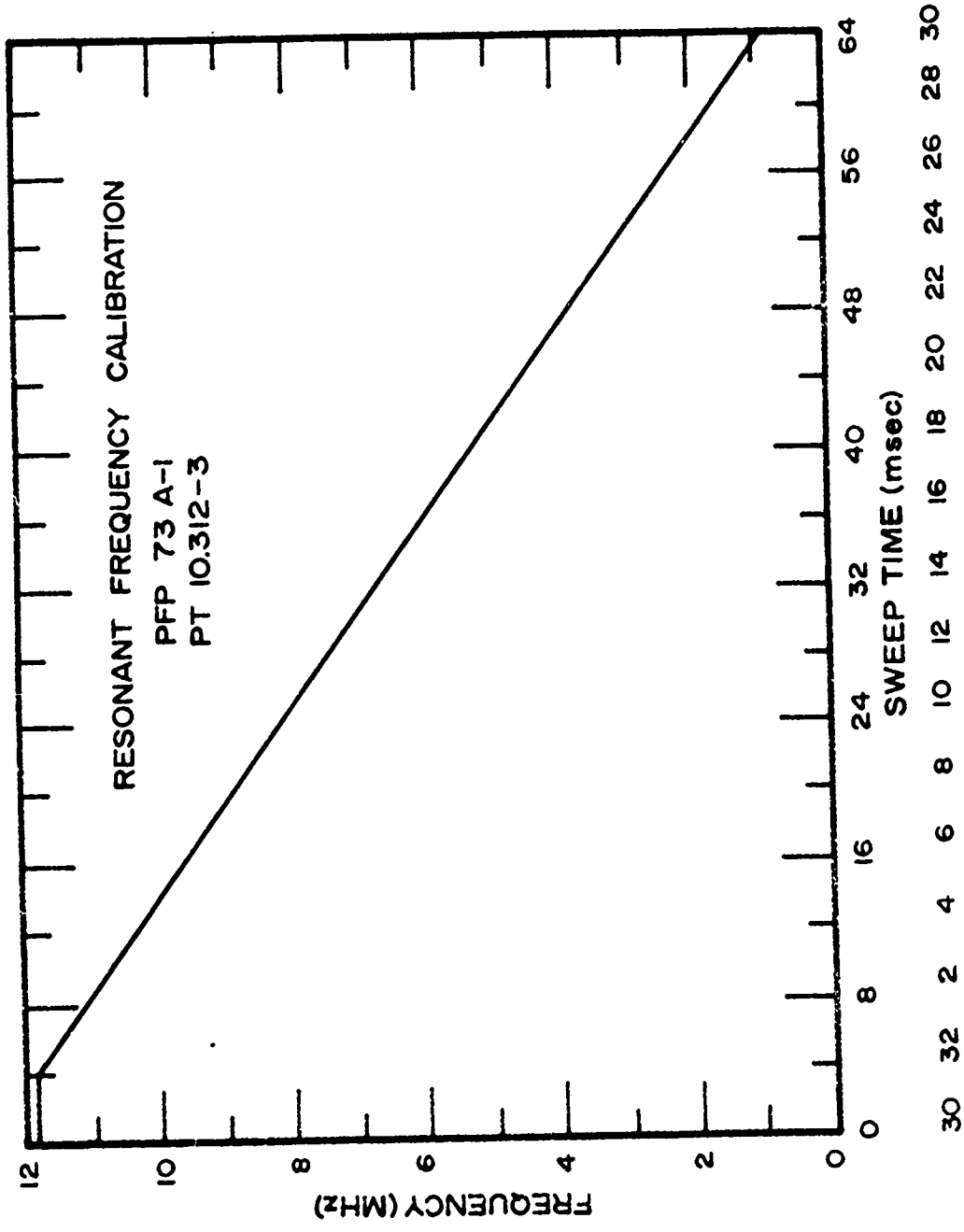

Figure A-17. Plasma frequency probe time of resonance vs. frequency.

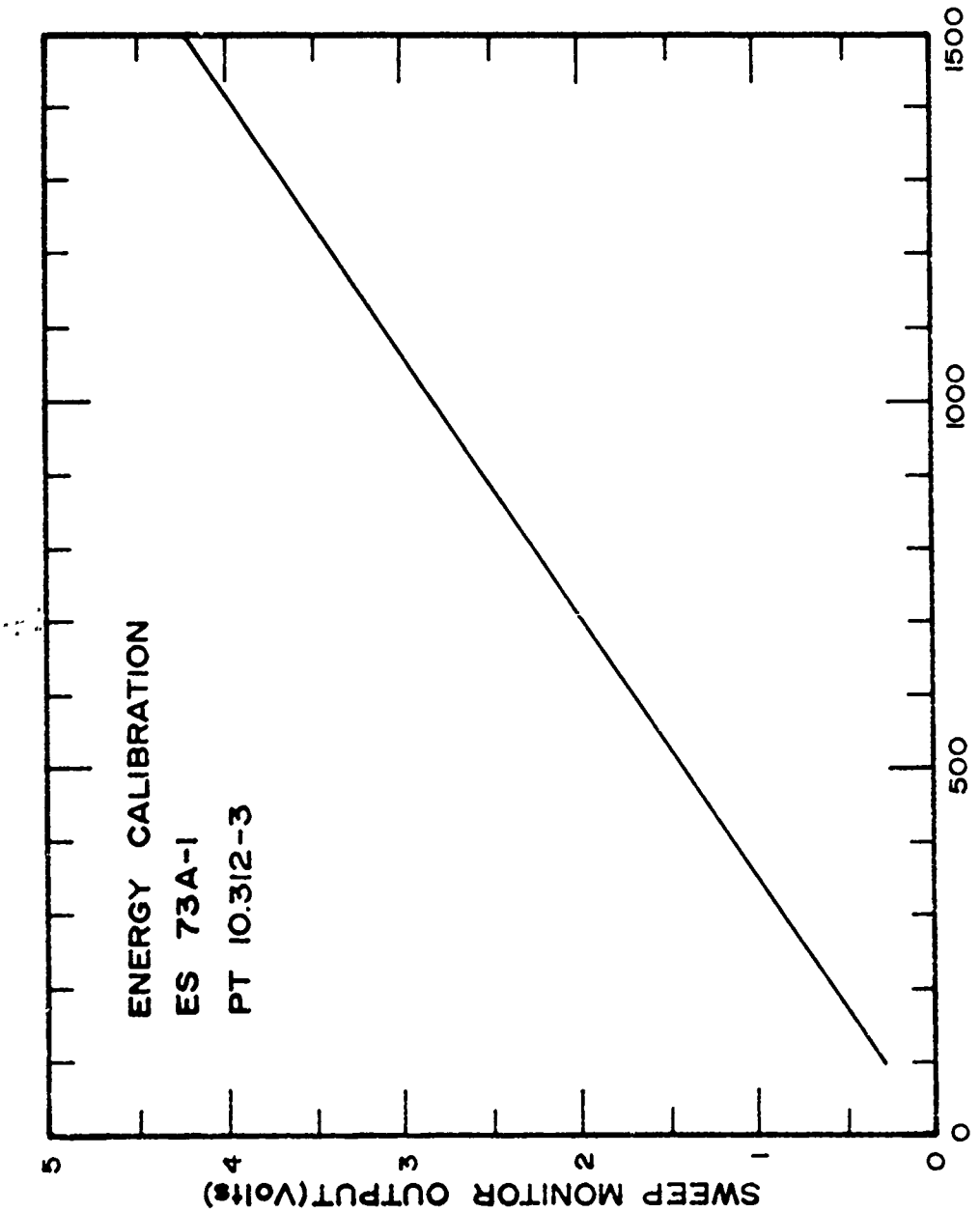

Figure A-18. Electron spectrometer energy calibration.

TABLE A-3

ELECTRON SPECTROMETER AMPLIFIER CALIBRATION DATA

Input (counts/second)	Output (volts)
1000	1.28
1500	1.78
2000	2.18
3000	2.75
4000	3.19
5000	3.52
6000	3.79
7000	4.02
8000	4.20
9000	4.37
10,000	4.50
11,000	4.62
12,000	4.74
13,000	4.83
14,000	4.92
15,000	5.01
16,000	5.07
17,000	5.07

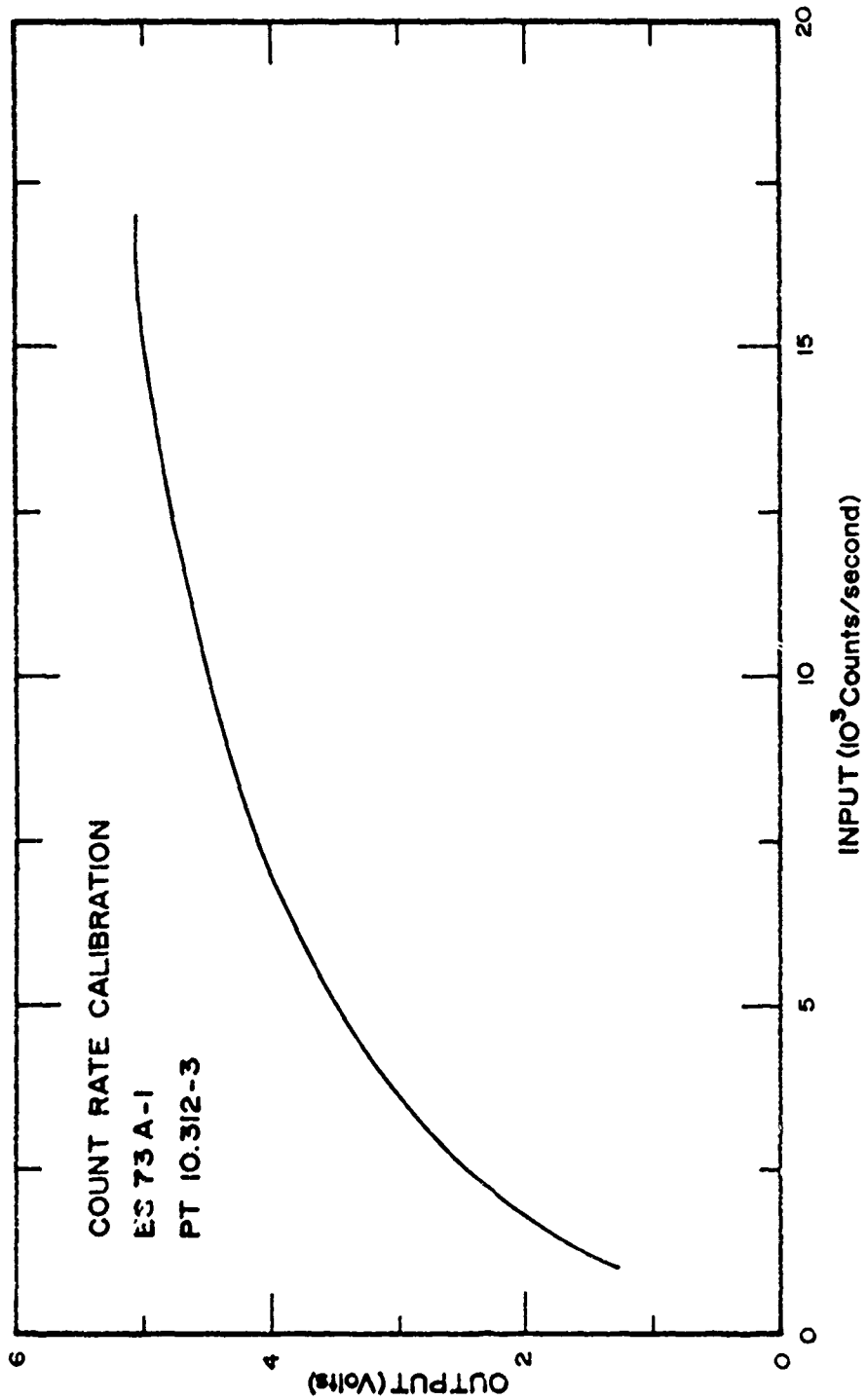

Figure A-19. Electron spectrometer count rate calibration.

TABLE A-4

PARTICLE COUNTER COMMUTATOR SEGMENT ASSIGNMENTS

Segment No.	Assignment	Segment No.	Assignment
13	+5 volts	5	9 kev electrons
14	+5 volts	6	4.5 kev electrons
15	+5 volts	7	28 kev electrons
16	0 volts	8	90 kev electrons
1	28 kev electrons	9	17 kev electrons
2	90 kev electrons	10	42 kev electrons
3	17 kev electrons	11	9 kev electrons
4	42 kev electrons	12	0 volts

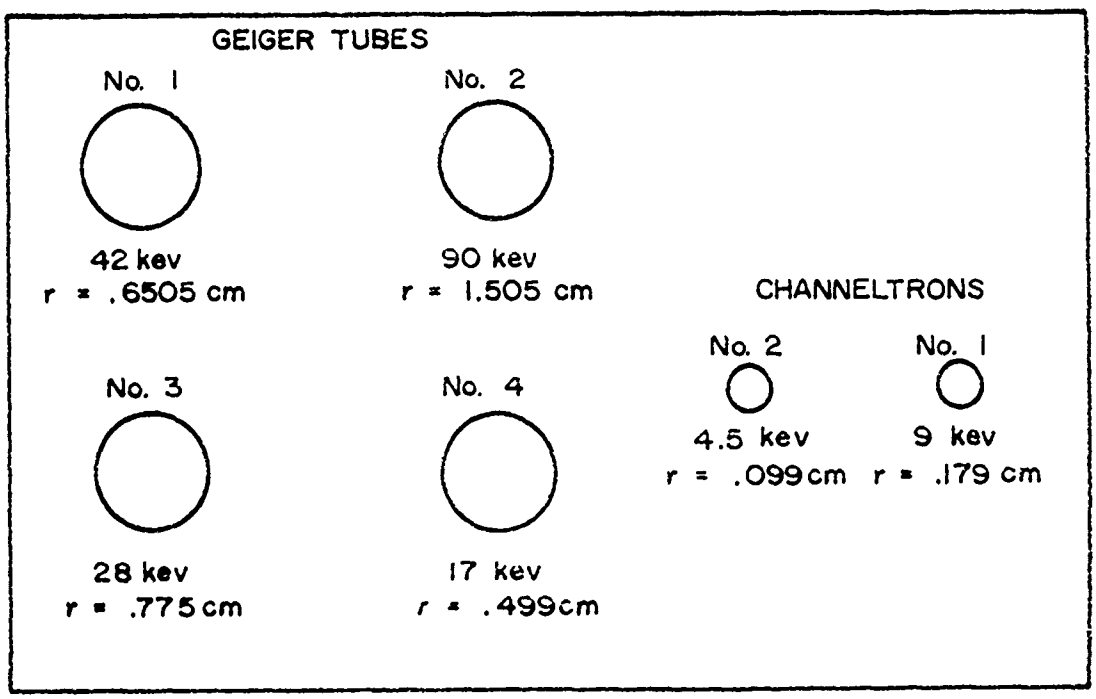

Figure A-20. Particle counter window locations.

TABLE A-5

PARTICLE COUNTER COUNT RATE CALIBRATION DATA

Input (Counts/sec)	Output (Volts) Elec ≥ 4.5 Kev	Elec ≥ 9 Kev	Elec ≥ 17 Kev	Elec ≥ 28 Kev	Elec ≥ 42 Kev	Elec ≥ 90 Kev
0	.04	.09	.06	.10	.08	.05
50	.29	.32	.33	.37	.35	.33
75	.44	.47	.50	.53	.52	.51
100	.58	.62	.67	.70	.68	.68
150	.81	.85	.92	.94	.93	.94
200	1.05	1.08	1.15	1.17	1.16	1.18
250	1.25	1.27	1.33	1.35	1.34	1.37
300	1.44	1.45	1.50	1.51	1.50	1.54
400	1.68	1.67	1.70	1.70	1.69	1.74
500	1.87	1.85	1.85	1.85	1.83	1.90
700	2.12	2.07	2.85	2.04	2.02	2.10
1000	2.37	2.30	2.26	2.25	2.22	2.32
1300	2.58	2.49	2.43	2.42	2.39	2.50
1600	2.76	2.66	2.60	2.58	2.55	2.67
2000	2.96	2.85	2.78	2.76	2.73	2.85
2500	3.16	3.04	2.97	2.95	2.91	3.04
3000	3.32	3.19	3.13	3.10	3.06	3.19
4000	3.54	3.41	3.55	3.32	3.27	3.41
5000	3.69	3.55	3.50	3.47	3.41	3.56
7000	3.89	3.75	3.71	3.68	3.61	3.77
9000	4.05	3.90	3.87	3.83	3.76	3.91
10000	4.11	3.96	3.94	3.90	3.82	3.98
12000	4.23	4.07	4.06	4.02	3.93	4.10
14000	4.34	4.17	4.17	4.12	4.03	4.20
16000	4.44	4.27	4.26	4.21	4.12	4.29
18000	4.53	4.36	4.36	4.31	4.21	4.38
20000	4.60	4.43	4.44	4.39	4.28	4.45
25000	4.75	4.58	4.60	4.54	4.44	4.62
30000	4.86	4.70	4.74	4.67	4.56	4.72
50000	5.00	4.91	4.98	4.93	4.81	4.95

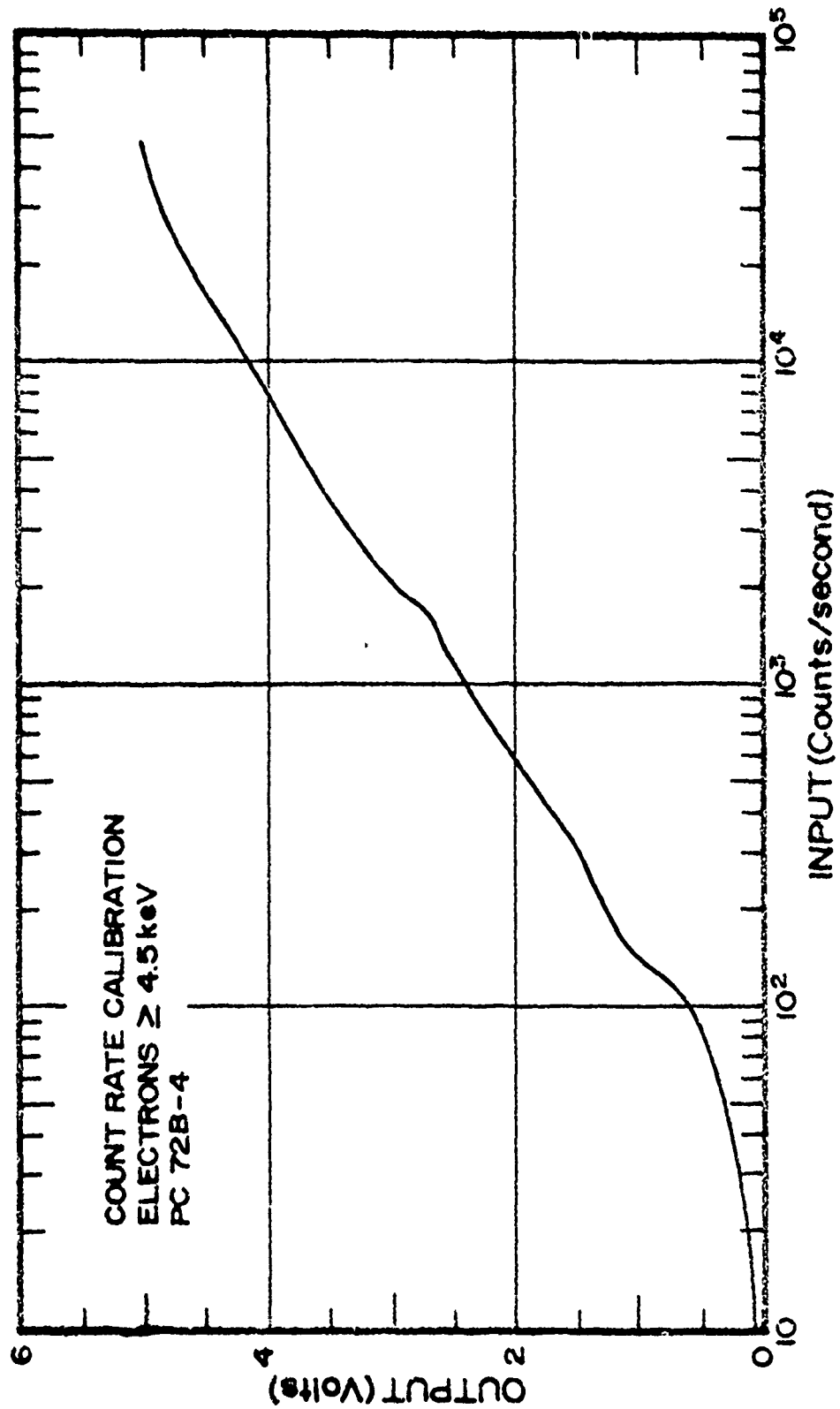

Figure A-21. Particle counter count rate calibration.

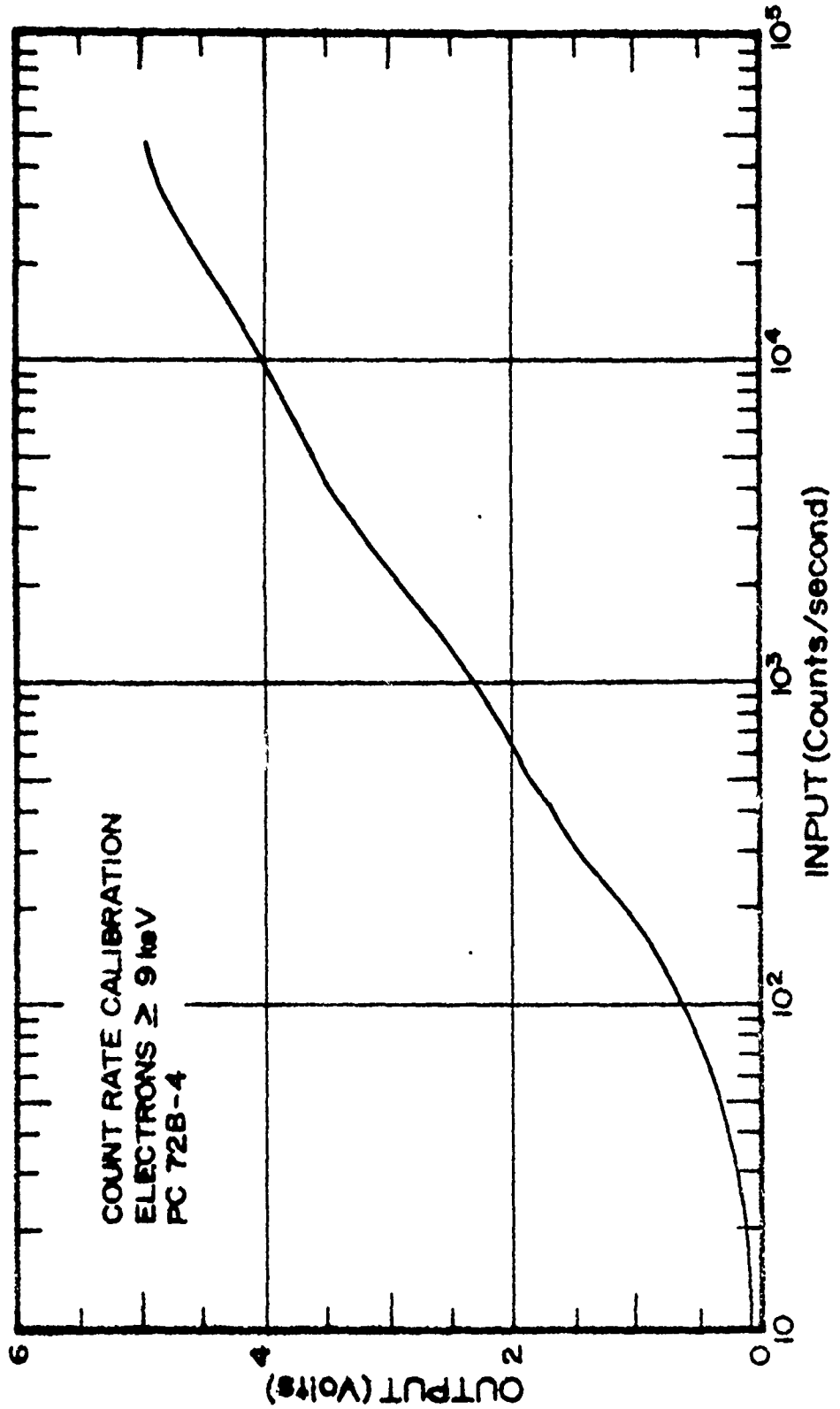

Figure A-22. Particle counter count rate calibration.

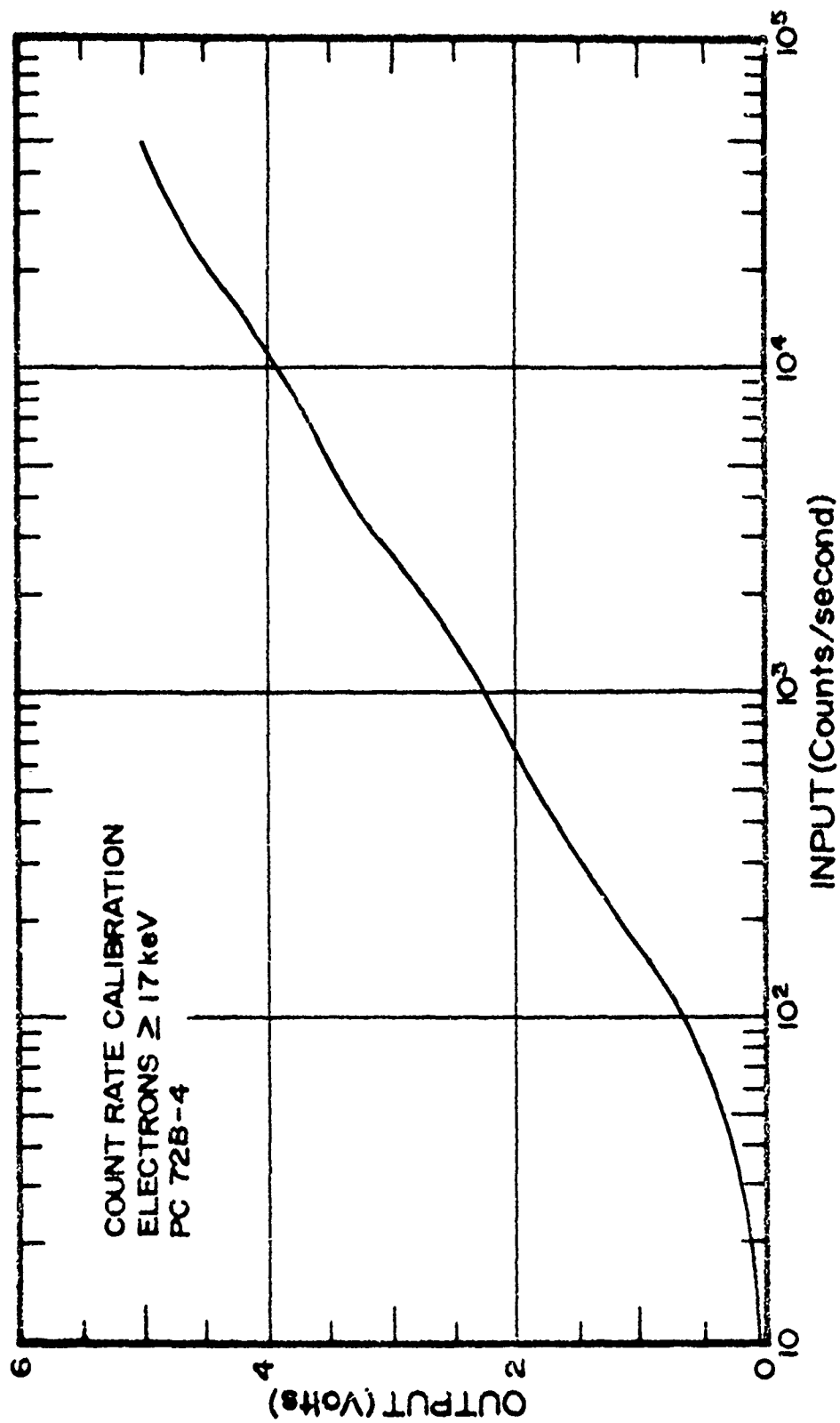

Figure A-23. Particle counter count rate calibration.

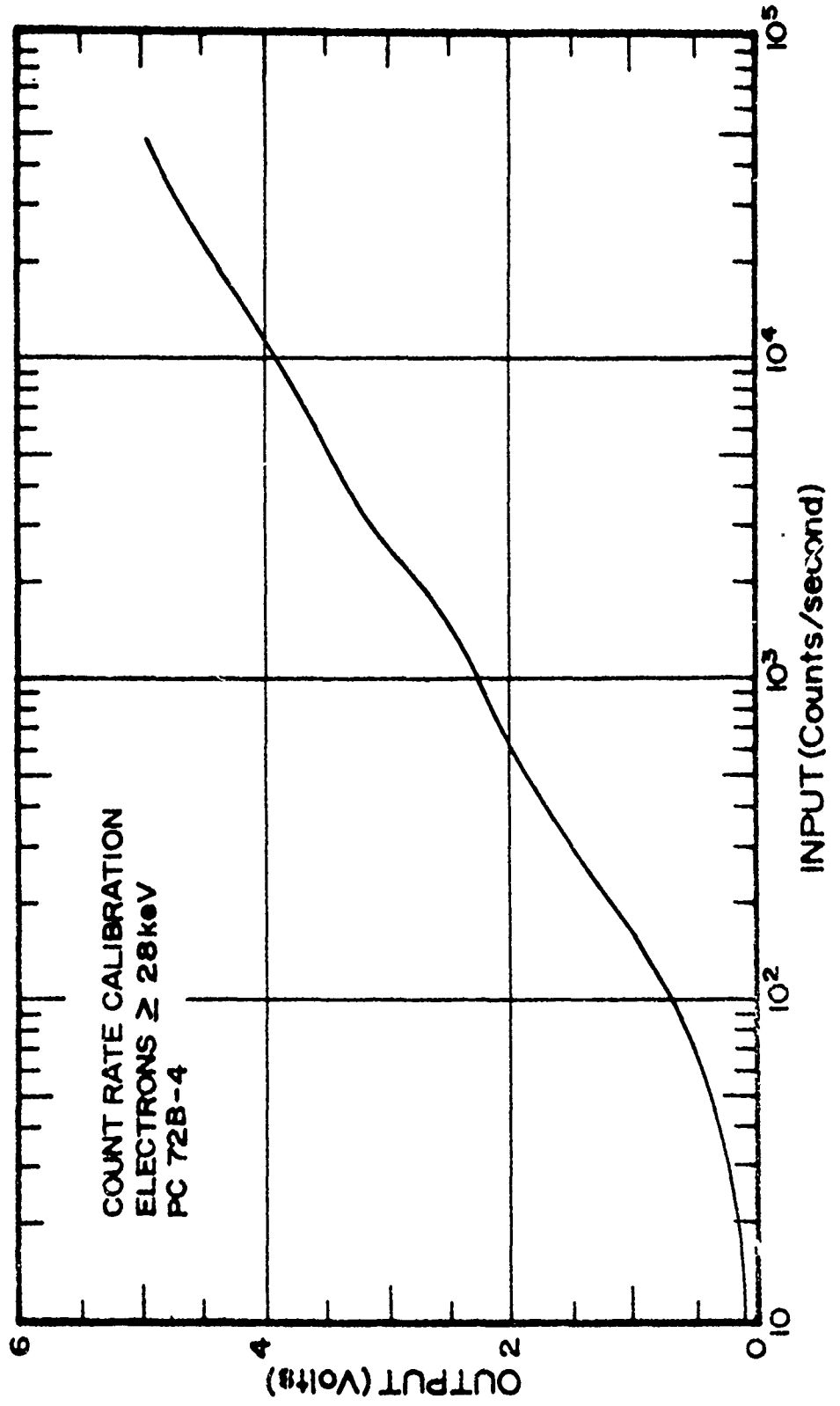

Figure A-24. Particle counter count rate calibration.

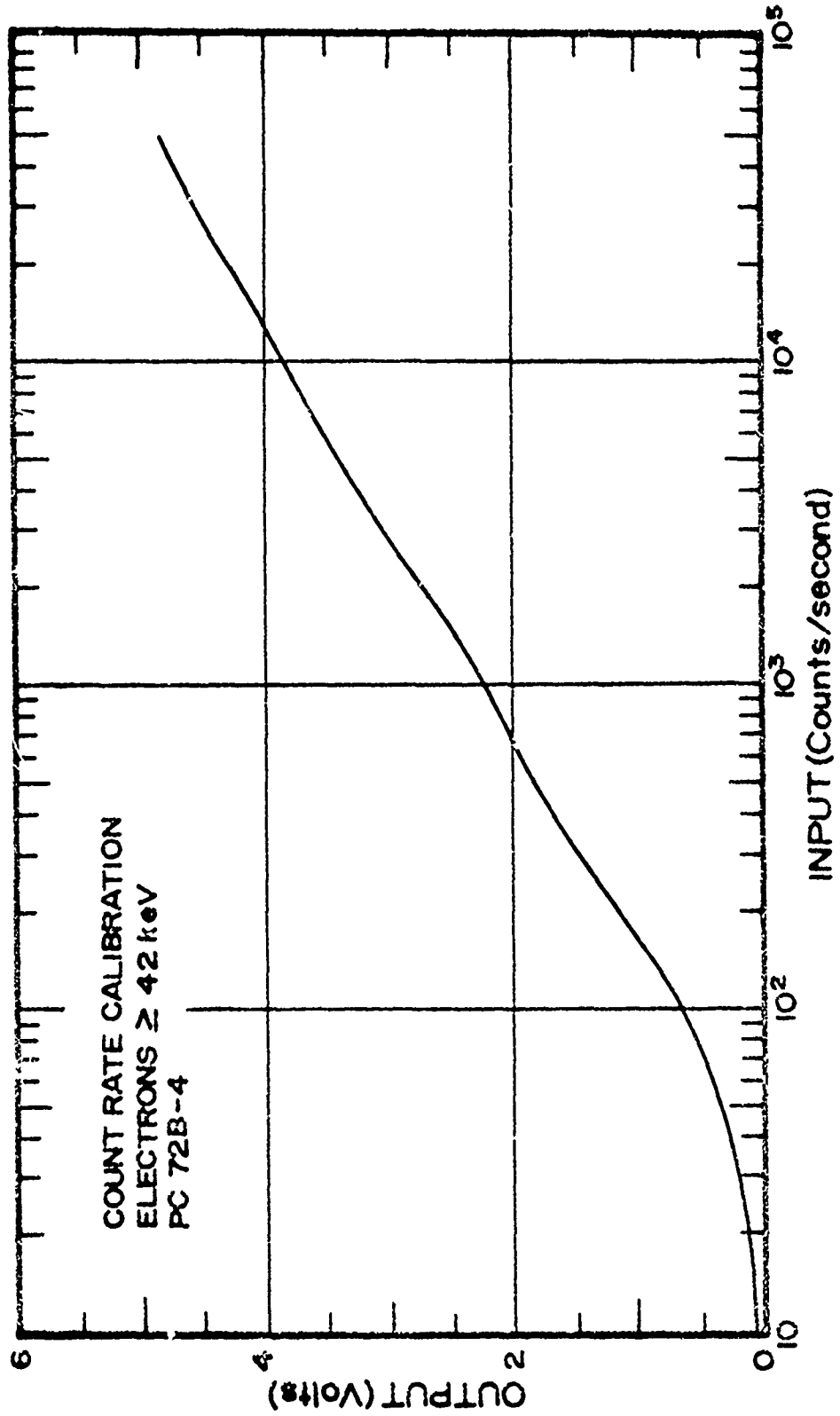

Figure A-25. Particle counter count rate calibration.

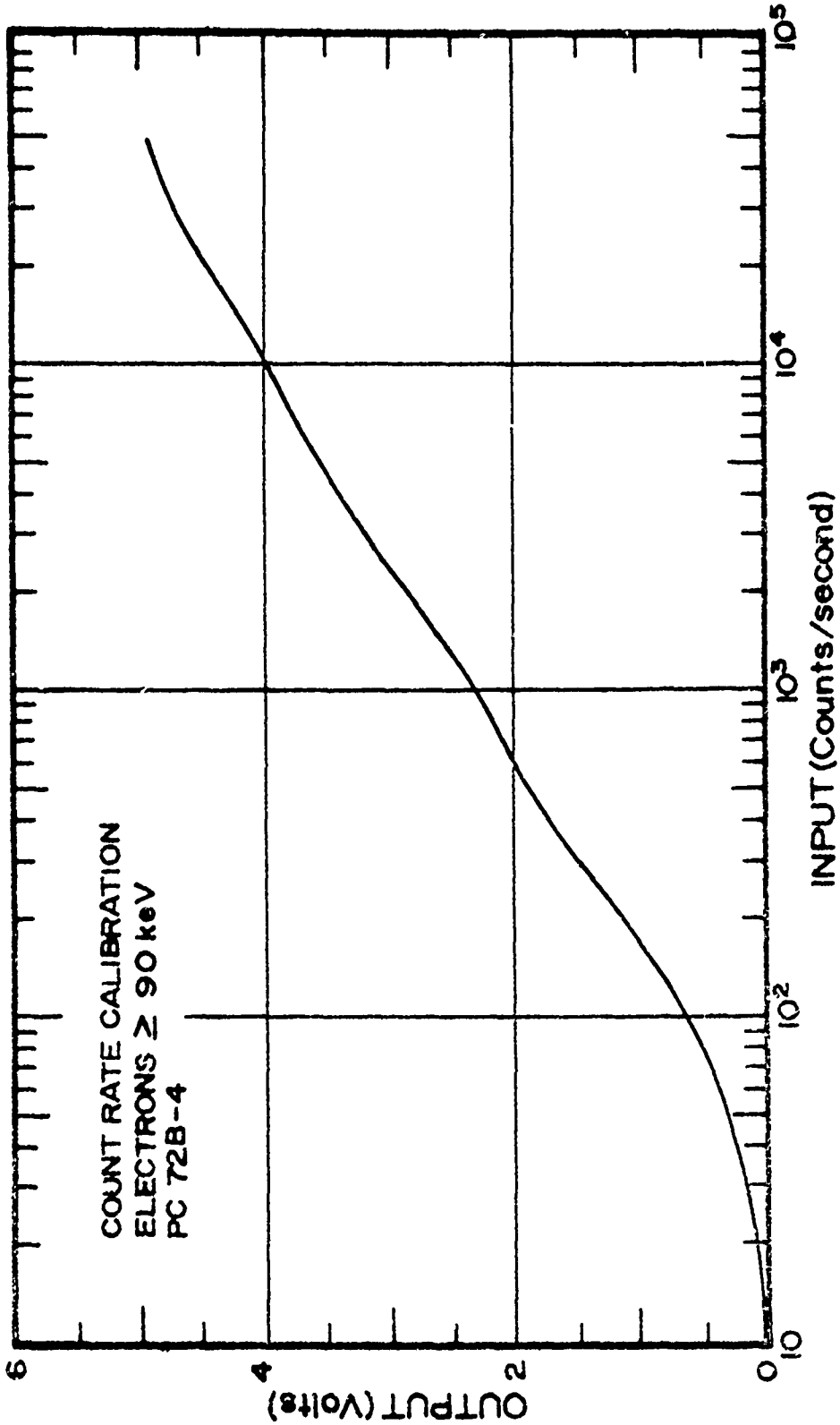

Figure A-26. Particle counter count rate calibration.

TABLE A-6

MAGNETIC ASPECT SENSOR CALIBRATION DATA

Field (Milligauss)		Output Signal (volts)
600		4.78
550		4.58
500		4.39
450		4.19
400		3.99
350		3.79
300		3.59
250		3.39
200		3.19
150		2.99
100		2.79
50		2.59
0	(Bias Level)	2.40
50		2.20
100		2.00
150		1.80
200		1.60
250		1.40
300		1.20
350		1.00
400		0.80
450		0.60
500		0.39
550		+0.19
600		-0.01

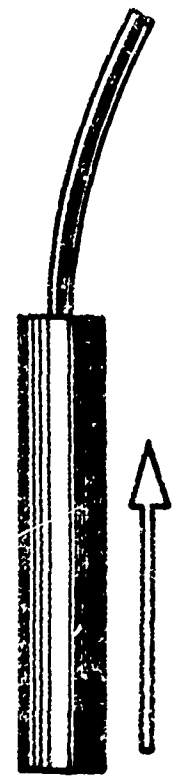

Direction of magnetic field for voltage signals above bias level.

APPENDIX B

TELEMETRY TECHNICAL DATA

TABLE B-1

PT 10.312-3 TELEMETRY ASSIGNMENTS

Trig Channel	Frequency (kHz)	Description
21	165	E-field Output (AC x 200)
20	124	LP Output (4 v Cal Pulse - 24 sec. interval)
19	93	PFP Output
18	70	Mides Gyro
17	52.5	E-field Output (DC x 2)
16	40	HARP Output (Digital)
15	30	ESA Sweep
14	22	E-field 10 x 30 Commutator
13	14.5	ESA Output
12	10.5	SES Log Rate Output (2.5 v Cal Pulse - 50 sec. interval)
11	7.35	PC Log Rate Output
10	5.4	1 x 60 Housekeeping Commutator
9	3.9	HARP Sweep Output
8	3.0	SES Sweep Output
7	2.3	LP Sweep Output
6	1.7	3914 A Photometer Output (4.5 v Cal Pulse - 30 sec. Interval)
5	1.3	Magnetometer Output

Note: Link No. 1 was used with a carrier frequency of 2279.5 Hz.

TABLE B-2

1 x 60 HOUSEKEEPING COMMUTATOR ASSIGNMENTS

Pin No.	Exp and/or Function	Note any special Voltage interpretation
1	2.5 v Cal	
2	0 v Cal	
3	ESA 28 v (delayed)	4 v=on, 0 v=off
4	ESA 28 v	≈ 4 v=on
5	ESA +15 v	3.75 v=on
6	ESA -15 v	2.5 v=on
7	ESA PMT H.V.	2.4=on (3 v with HV off)
8	ESA Accel H.V.	2.5 v=on, 0 v=off
9	ESA Cover Mon.	4.5 v=on
10	ESA Temp Mon.	2 v=Room Temp
11	0 v Cal.	
12	PC Channeltron H.V.	3.5 v=on, 0 v=off
13	PC Geiger H.V.	2 v=on
14	0 v	
15	0 v	
16	0 v H.V. Mon.	2.2 v=on
17	0 v	
18	Main Door Mon.	3.7 v=off, 1 v=on
19	SES Platform Mon.	1 v=in, 3.7 = out
20	PFP Door Mon.	3.7 v=door on
21	N.T. Mon.	1.6 v=off, .5 v=on
22	0 v	
23	28 v Mon.	2.75 v = 32 v

TABLE B-2 (cont.)

Pin No.	Exp and/or Function	Note any special Voltage interpretation.
24	Pyro Prim Mon.	2.3 v = 16 v
25	Pyro Sec. Mon.	2.3 v = 16 v
26	0 v	
27	0 v	
28	0 v	
29	0 v	
30	0 v	
31	ESA 28 v (HV delayed)	
32	ESA 28 v	
33	ESA + 15 v	
34	ESA - 15 v	
35	ESA PMT HV	
36	ESA Accel. HV	
37	ESA Cover Mon.	
38	ESA Temp. Mon.	
39	0 v	
40	PC Channeltron HV	
41	PC Geiger HV	
42	0 v	
43	3914 A Temp. Mon	
44	3914 A HV Mon.	
45	0 v	
46	Main Door Mon.	
47	SES Platform Mon.	

TABLE B-2 (cont.)

Pin No.	Exp and/or Function	Note any special Voltage interpretation
48	PFP Door Mon.	
49	NT Mon.	
50	0 v	
51	+28 v batt.	
52	Pyro Prim Mon.	
53	Pyro Sec. Mon.	
54	0 v	
55	0 v	
56	0 v	
57	5 v	
58	5 v	
59	5 v	
60	0 v	

TABLE C-1

PT 10.312-3 TRAJECTORY LISTING

Time (sec)	Altitude (km)	Velocity (km/sec)	Time (sec)	Altitude (km)	Velocity (km/sec)
13	7.013	.477	43	45.358	1.633
14	7.480	.466	44	46.978	1.626
15	7.942	.460	45	48.590	1.618
16	8.391	.437	46	50.195	1.610
17	8.814	.413	47	51.790	1.598
18	9.215	.393	48	53.371	1.583
19	9.624	.442	49	54.940	1.574
20	10.131	.579	50	56.510	1.566
21	10.769	.700	51	58.056	1.559
22	11.545	.869	52	59.598	1.546
23	12.493	1.020	53	61.129	1.535
24	13.587	1.196	54	62.650	1.526
25	14.880	1.379	55	64.163	1.518
26	16.332	1.548	56	65.667	1.510
27	17.995	1.705	57	67.163	1.510
28	19.713	1.809	58	68.647	1.488
29	21.519	1.808	59	70.120	1.475
30	23.320	1.800	60	71.581	1.466
31	25.088	1.754	61	73.035	1.459
32	26.832	1.752	62	74.481	1.451
33	28.574	1.746	63	75.919	1.443
34	30.306	1.733	64	77.348	1.433
35	32.025	1.718	65	78.767	1.422
36	33.729	1.706	66	80.173	1.408
37	35.424	1.697	67	81.568	1.399
38	37.108	1.688	68	82.955	1.394
39	38.782	1.677	69	84.335	1.385
40	40.444	1.665	70	85.705	1.376
41	42.094	1.652	71	87.066	1.366
42	43.730	1.641	72	88.417	1.354

TABLE C-1 (cont.)

Time (sec)	Altitude (km)	Velocity (km/sec)	Time (sec)	Altitude (km)	Velocity (km/sec)
73	89.754	1.342	104	126.609	1.049
74	91.084	1.336	105	127.643	1.042
75	92.407	1.330	106	128.670	1.035
76	93.722	1.319	107	129.689	1.026
77	95.026	1.308	108	130.697	1.016
78	96.319	1.298	109	131.697	1.009
79	97.602	1.286	110	132,688	.999
80	98.873	1.276	111	133.669	.988
81	100.136	1.269	112	134.638	.977
82	101.392	1.262	113	135.597	.969
83	102.640	1.252	114	136.549	.962
84	103.878	1.243	115	137.493	.953
85	105.107	1.234	116	138.426	.942
86	106.326	1.222	117	139.349	.932
87	107.532	1.211	118	140.264	.925
88	108.727	1.202	119	141.172	.916
89	109.915	1.195	120	142.069	.906
90	111.095	1.186	121	142.955	.894
91	112.265	1.177	122	143.831	.834
92	113.426	1.168	123	144.696	.876
93	114.577	1.158	124	145.554	.870
94	115.716	1.145	125	146.404	.861
95	116.843	1.133	126	147.244	.849
96	117.961	1.127	127	148.073	.839
97	119.075	1.122	128	148.893	.832
98	120.183	1.114	129	149.705	.823
99	121.281	1.102	130	150.509	.815
100	122.367	1.091	131	151.303	.804
101	123.442	1.062	132	152.085	.792
102	124.509	1.073	133	152.856	.783
103	125.565	1.061	134	153.620	.775

TABLE C-1 (cont.)

Time (sec)	Altitude (km)	Velocity (km/sec)	Time (sec)	Altitude (km)	Velocity (km/sec)
135	154.376	.768	166	173.168	.490
136	155.125	.760	167	173.627	.479
137	155.864	.748	168	174.075	.468
138	156.590	.738	169	174.514	.460
139	157.306	.730	170	174.945	.452
140	158.014	.721	171	175.357	.443
141	158.711	.713	172	175.777	.434
142	159.403	.704	173	176.178	.421
143	160.085	.694	174	176.570	.419
144	160.757	.683	175	176.954	.410
145	161.417	.673	176	177.327	.401
146	162.067	.664	177	177.691	.394
147	162.708	.655	178	178.046	.388
148	163.341	.648	179	178.390	.378
149	163.966	.641	180	178.723	.366
150	164.584	.632	181	179.045	.354
151	165.191	.622	182	179.358	.346
152	165.787	.612	183	179.667	.339
153	166.375	.602	184	179.969	.332
154	166.954	.594	185	180.262	.321
155	167.523	.586	186	180.543	.309
156	168.085	.578	187	180.813	.300
157	168.638	.568	188	181.073	.293
158	169.181	.558	189	181.327	.291
159	169.712	.547	190	181.577	.289
160	170.232	.537	191	181.818	.285
161	170.744	.530	192	182.048	.276
162	171.247	.521	193	182.264	.265
163	171.741	.511	194	182.467	.254
164	172.223	.502	195	182.658	.245
165	172.699	.497	196	182.840	.239

TABLE C-1 (cont.)

Time (sec)	Altitude (km)	Velocity (km/sec)	Time (sec)	Altitude (km)	Velocity (km/sec)
197	183.016	.236	228	183.949	.185
198	183.184	.232	229	183.834	.185
199	183.346	.222	230	183.711	.188
200	183.499	.210	231	183.581	.194
201	183.644	.200	232	183.441	.202
202	183.779	.195	233	183.290	.214
203	183.904	.192	234	183.127	.226
204	184.017	.190	235	182.952	.237
205	184.119	.188	236	182.766	.245
206	184.209	.183	237	182.650	.252
207	184.291	.174	238	182.364	.260
208	184.365	.169	239	182.150	.266
209	184.431	.172	240	181.929	.270
210	184.438	.178	241	181.701	.274
211	184.536	.178	242	181.468	.280
212	184.576	.171	243	181.227	.288
213	184.605	.165	244	180.974	.300
214	184.624	.161	245	180.708	.313
215	184.632	.156	246	180.428	.324
216	184.633	.153	247	180.137	.332
217	184.625	.154	248	179.838	.338
218	184.611	.155	249	179.534	.344
219	184.589	.156	250	179.224	.350
220	184.559	.158	251	178.906	.359
221	184.519	.164	252	178.578	.369
222	184.467	.172	253	178.237	.378
223	184.404	.175	254	177.845	.385
224	184.332	.175	255	177.526	.391
225	184.250	.176	256	177.161	.398
226	184.158	.180	257	176.787	.408
227	184.058	.183	258	176.403	.420

TABLE C-1 (cont.)

Time (sec)	Altitude (km)	Velocity (km/sec)	Time (sec)	Altitude (km)	Velocity (km/sec)
259	176.006	.431	290	159.078	.703
260	175.599	.439	291	158.425	.713
261	175.183	.446	292	157.723	.724
262	174.759	.456	293	157.012	.733
263	174.324	.466	294	156.291	.743
264	173.880	.474	295	155.558	.754
265	173.425	.484	296	154.815	.765
266	172.967	.491	297	154.062	.774
267	172.476	.502	298	153.300	.782
268	172.014	.511	299	152.529	.791
269	171.523	.518	300	151.750	.799
270	171.026	.525	301	150.962	.808
271	170.518	.536	302	150.164	.817
272	169.998	.545	303	149.357	.826
273	169.470	.551	304	148.541	.834
274	168.973	.557	305	147.718	.841
275	168.395	.566	306	146.887	.849
276	167.843	.576	307	146.046	.860
277	167.282	.584	308	145.193	.873
278	166.712	.593	309	144.327	.885
279	166.132	.604	310	143.452	.893
280	165.541	.615	311	142.569	.901
281	164.940	.624	312	141.677	.909
282	164.330	.632	313	140.777	.918
283	163.711	.641	314	139.867	.927
284	163.083	.651	315	138.948	.934
285	162.444	.661	316	138.023	.942
286	161.796	.669	317	137.089	.950
287	161.139	.677	318	136.147	.960
288	160.474	.686	319	135.193	.970
289	159.800	.695	320	134.229	.981

TABLE C-1 (cont.)

Time (sec)	Altitude (km)	Velocity (km/sec)	Time (sec)	Altitude (km)	Velocity (km/sec)
321	133.254	.991	352	98.230	1.281
322	132.270	1.000	353	96.995	1.288
323	131.277	1.010	354	95.672	1.296
324	130.273	1.020	355	94.379	1.306
325	129.259	1.029	356	93.007	1.317
326	128.238	1.036	357	91.763	1.329
327	127.210	1.044	358	90.457	1.340
328	126.171	1.059	359	89.101	1.349
329	125.117	1.067	360	87.757	1.357
330	124.048	1.090	361	86.404	1.367
331	122.968	1.098	362	85.041	1.377
332	121.880	1.106	363	83.669	1.385
333	120.783	1.115	364	82.288	1.395
334	119.676	1.126	365	80.897	1.403
335	118.559	1.135	366	79.502	1.400
336	117.443	1.144	367	78.110	1.399
337	116.299	1.152	368	76.710	1.416
338	115.157	1.158	369	75.287	1.442
339	114.009	1.161	370	73.846	1.456
340	112.854	1.169	371	72.397	1.457
341	111.689	1.181	372	70.951	1.449
342	110.513	1.193	373	69.510	1.445
343	109.325	1.203	374	68.065	1.459
344	108.124	1.212	375	66.548	1.489
345	106.923	1.220	376	65.104	1.514
346	105.710	1.228	377	63.594	1.520
347	104.488	1.236	378	62.086	1.512
348	103.258	1.245	379	60.582	1.512
349	102.016	1.257	380	59.068	1.534
350	100.765	1.269	381	57.529	1.562
351	99.500	1.276	382	55.813	1.573

TABLE C-1 (cont.)

Time (sec)	Altitude (km)	Velocity (km/sec)	Time (sec)	Altitude (km)	Velocity (km/sec)
383	54.407	1.568	414	18.793	.247
384	52.852	1.557	415	18.557	.236
385	51.308	1.544	416	18.329	.229
386	49.778	1.529	417	18.106	.224
387	48.254	1.535	418	17.886	.221
388	46.711	1.518	419	17.669	.217
389	45.136	1.596	420	17.459	.206
390	43.553	1.588	421	17.252	.192
391	41.988	1.563	422	17.078	.182
392	40.444	1.548	423	16.899	.180
393	38.908	1.543	424	16.720	.179
394	37.381	1.527	425	16.544	.175
395	35.880	1.490	426	16.372	.172
396	34.417	1.448	427	16.200	.174
397	32.994	1.409	428	16.026	.174
398	31.610	1.365	429	15.854	.171
399	30.274	1.313	430	15.687	.165
400	28.989	1.265	431	15.524	.162
401	27.746	1.230	432	15.363	.161
402	26.540	1.189	433	15.202	.161
403	25.388	1.116	434	15.041	.161
404	24.327	1.009	435	14.880	.161
405	23.381	.888	436	14.721	.158
406	22.550	.778	437	14.566	.152
407	21.820	.689	438	14.416	.149
408	21.172	.615	439	14.267	.151
409	20.594	.546	440	14.114	.154
410	20.088	.469	441	13.959	.155
411	19.965	.386	442	13.805	.154
412	19.323	.314	443	13.651	.154
413	19.042	.268	444	13.498	.154

TABLE C-1 (cont.)

Time (sec)	Altitude (km)	Velocity (km/sec)
445	13.344	.153
446	13.192	.153
447	13.038	.154
448	12.885	.153
449	12.732	.153
450	12.579	.154

APPENDIX D

HIGH ALTITUDE EFFECTS SIMULATION (HAES)

PROGRAM REPORTS

TABLE D-1

HAES REPORT LIST

HAES Report 1

Rocket Launch of a SWIR Spectrometer into an Aurora (ICECAP 72).
D.J. Baker, C.L. Wyatt, W.R. Pendelton, Jr., - Utah State,
J.C. Ulwick - AFCRL; AFCRL-TR-74-0077, February 1974.

HAES Report 2

Analysis of HAES Results: ICECAP 72.
W.P. Reidy, T.C. Degges, O.P. Manley, H.J. Smith, J.W. Carpenter-Visidyne, A.T. Stair, J.C. Ulwick - AFCRL, D.J. Baker - Utah State;
DNA 3247F, April 1974.

HAES Report 3

Rocket Instrumentation for ICECAP 73A, Auroral Measurements Program - Black Brant 18.205-1.
D.A. Burt, C.S. Davis - Utah State, AFCRL-TR-74-0195, February 1974.

HAES Report 4

Data Reduction and Auroral Characterization for ICECAP.
I. Kofsky - Photometrics, DNA 3511F, January 1975.

HAES Report 5

ICECAP Analysis: Energy Deposition and Transport in the Auroral Ionosphere.
R.D. Sears - LMSC, DNA 3566F, November 1974

HAES Report 6

Auroral Simulation Studies
D. Archer - MRC, DNA 3367T

HAES Report 7

ICECAP 72- Rocket Measurement Program for Investigation of Auroral IR Emissions - Black Brant 17.110-3.

D.A. Burt, G.D. Allred, J.C. Kemp, L.C. Howlett, E.F. Pound, G.K. LeBaron - Utah State, AFCRL-TR-75-0001, September 1974.

HAES Report 8

Design and Calibration of a Rocket-Borne Electron Spectrometer.
P.C. Neal, AFCRL-TR-74-0629, December 1974.

HAES Report 9

Near Infrared Auroral Spectra.
D. Baker, A. Steed, R. Huppi, AFCRL-TR-75-0010, December 1974.

HAES Report 10

Arctic Code Electron Deposition Theory with Application to Project Excede.
P.W. Tarr-MRC, MRC-R-173, February 1975.

HAES Report 11

Rocketborne Instrumentation for the Measurement of Electric Fields - Paiute Tomahawk 10.312-3.
L.C. Howlett, R.J. Bell - Utah State, AFCRL-TR-75-0023, Sci. Rpt. 2, January 1975.